A Comparison of Bayesian Inference Strategies for Parameterisation of Large Amplitude AC Voltammetry Derived From Total Current and Fourier Transformed Versions*

Luke Gundry[1], Dr. Gareth Kennedy[1], Prof. Jonathan Keith[2], Dr. Martin Robinson[3], Prof. David Gavaghan[3], Prof. Alan M. Bond*[1], and Prof. Jie Zhang*[1]

[1]School of Chemistry, Monash University, Clayton, Vic. 3800, Australia
[2]School of Mathematics, Monash University, Clayton, Vic. 3800, Australia.
[3]Department of Computer Science, University of Oxford, Wolfson Building, Parks Road, Oxford, OX1 3QD, United Kingdom.
[1]Email: Alan.Bond@monash.edu, Jie.Zhang@monash.edu

July 20, 2021

Abstract

Use of carefully designed computer supported parameterisation methods in voltammetric studies can provide highly robust and accurate methods for simultaneously quantifying the large number of parameters present in complex electrochemical reactions. In this study, a computer program has been developed to parameterise large amplitude AC voltammetric data using mathematical optimisation in combination with Bayesian inference algorithms for calculating posterior distributions of parameters and hence uncertainties in parameter values. The computer program has been applied to objective functions, relevant to total AC current, frequency domain data in the form of the power spectrum derived from Fourier transformation and multivariate based methods using the resolved harmonic data. The robustness of the objective functions have been confirmed and Bayesian inference methods have been validated using "noisy" synthetic and experimental data for the $[Fe(CN)_6]^{3-/4-}$ reduction process in aqueous 3.0 M KCl electrolyte at a gold electrode. It was found that the harmonic based Bayesian inference methods outperformed other methods in parameterisation of the thermodynamics and electrode kinetics of the close to reversible $[Fe(CN)_6]^{3-/4-}$ process due to their ability to compensate for non-ideality in the modelling and the superior parameter sensitivities available in the higher harmonics. The computer supported and heuristic methods were compared. Their advantages and limitations were discussed.

*This paper is dedicated to the memory of Jean-Michel Savéant.

1 Introduction

In the past few decades, voltammetry has evolved into a powerful tool for the quantitative investigation and understanding of chemically and biologically important processes. Pioneering work by outstanding electrochemists such as Jean-Michel Savéant [1] has inspired much of the current research activity in this field. Obtaining quantitative thermodynamic, kinetic, and mass transport information is a major prerequisite for understanding the significance of voltammetric data. [1–3] Occasionally, this can be achieved by comparing experimental data to that obtained by an analytical solution to the theory. For example, in the case of a reversible (Nernstian) process, and assuming the impact of uncompensated resistance (R_u) is insignificant, the Randles-Sevcik equation [2] can be used to calculate the diffusion coefficient (D), from the peak current obtained in linear sweep relevant voltammetry, provided the electrode area (A_{we}), the concentration (C) of the electroactive species and other parameters are known. However, in most cases, analytical solutions that describe the theory are not available and numerical simulations of models proposed to mimic the experimental data are employed. Nowadays, user friendly commercially available dedicated voltammetric simulation software packages, such as DigiSim®, [4] DigiElch® and KISSA-1D [5] are available to users of the technique who may not be familiar with the mathematics that underpin the models or do not wish to develop the often extensive computer code needed to solve the relevant differential equations. If an electrochemist wishes to write their own software to solve the differential equations that underpin the theory of voltammetry, then using code provided by MATLAB, Wolfram Mathematica or COMSOL Multiphysics® can be very useful. In particular, when the electrode geometry is complicated or the electrochemical process is governed by physical/chemical principles with a higher level of complexity, the powerful COMSOL Multiphysics® software is commonly used to solve the problem using a finite element method. [6] Other simulation packages such as the Monash Electrochemistry Simulator (MECSim), [7] which is used in this study, can be downloaded free of charge from the Internet. MECSim, emphasises the technique of AC voltammetry and has the ability to facilitate the simulation of a wide range of models in what is known as the forward problem. Like some commercially available software [4] it also provides access to computer supported parameter optimisation of the models in which the set of parameters that gives the best agreement between experiment and simulated data is identified in what is known as the inverse problem. [8–10]

Traditionally, the inverse problem in voltammetry has been solved heuristically using visually based trial and error comparisons of experimental and simulated data, which is tedious, time-consuming, lacks a statistical basis and is prone to bias.[7,11] Furthermore, even an experienced researcher will struggle to quantify more than three unknown parameters simultaneously using this method. Whereas, models in voltammetric simulations usually require a much wider range of parameters with different degrees of uncertainty. For example, models for a quasi-reversible electron transfer reaction include charge transfer rate constant (k^0) and charge transfer coefficient (α) when Butler-Volmer theory applies,[2] the reversible potential (E^0), D, R_u, the double layer capacitance (C_{dl}) and A_{we}, together with parameters whose values are assumed to be accurately known, such as temperature (T), C and scan rate (ν) in the case of DC voltammetry.

The first task in the heuristic method is primarily to pre-determine as many parameters in the model as possible and then vary the remaining ones, until the simulation provides an acceptable match with the experimental data. In the case of quantitative studies by DC cyclic voltammetry, a scenario for the heuristic parameterisation of a quasi-reversible electrode process may be as follows: R_u and C_{dl} are calculated from the R_uC_{dl} time constant using data where no faradaic current is present; E^0 is approximated as the mid point potential derived from the oxidation and reduction peak potentials assuming the diffusion coefficients for the oxidised and reduced forms are comparable and A_{we} is determined using voltammetric data derived from a species with a known D value that undergoes a reversible electron transfer process. Once this preliminary series of exercises has been completed, the still unknown k^o, α and D values need be varied in simulations. The experimenter then provide estimates of these parameter values by achieving what is perceived to be satisfactory agreement between experimental and simulated data.

To overcome the drawbacks associated with the heuristic method, highly efficient and robust automated parameter identification methods based on data optimisation have been employed taking advantage of rapidly increasing computing power.[8,12–14] Of particular relevance to the present study, Bayesian inference methods using the Markov Chain Monte Carlo (MCMC) method have been introduced for parameter quantification with uncertainty estimation in DC and AC voltammetry.[15,16] Due to the time series structure of the experimental data and the need to quantify parameters from comparison to simulated data, these and other forms of dynamic voltammetry are naturally suited for implementing data analysis in a Bayesian framework. The

Bayesian approach provides a posterior probability distribution for a parameter derived from the experimental data in a format known as a sampled from the posterior distribution.[17] The calculation initially assumes a uniform prior distribution, although other prior distributions are possible, to calculate the posterior distribution as a basis for statistical inference. Bayesian inference methods provide automatic identification of multiple parameters in a statistical framework when experimental and simulated data are compared. That is, the Bayesian outcome provides not only a best fit for the parameters but also the uncertainty of the parameters and identifies the extent of the correlation between them.

The Bayesian inference data analysis method has been applied to the form of AC voltammetry in which a large amplitude sinusoidal waveform with a given amplitude (ΔE) and a frequency (f) is superimposed on the ramped potential used in DC voltammetry and the total current (AC plus DC) is measured as a function of DC potential or time (Figures 1a and 1b, respectively). The application of Bayesian inference to the total current dataset allows the uncertainties in parameter estimates to be established.[15,16] However, the resultant total current-time data can also be transformed into the frequency domain using Fourier transformation which resolves the aperiodic DC component near zero frequency and AC harmonic components at integer multiples of the frequency of the applied sine wave (f, $2f$, $3f$, etc). Windowing and filtering followed by use of an inverse Fourier transformation provide the resolved DC and AC harmonics in the time domain.[18,19] This form of AC voltammetry is called Fourier transformed AC (FTAC) voltammetry, a technique that has been developed and applied widely in its large amplitude form by the Monash Electrochemistry Group and is attracting increased attention by others in recent times.[20–26] The FTAC voltammetric data processing procedure is schematically shown in Figure 1.

Importantly and uniquely in the field of voltammetry, the background current in FTAC voltammetry is only significant in the DC and fundamental AC harmonic and minimal (ideally zero) in the second and higher order harmonics. Thus, resolved and close to purely faradaic second and higher order AC harmonic data sets become available from a single experiment as does the aperiodic DC and fundamental harmonic data containing a mixture of faradaic and capacitance current. Furthermore, the DC and each AC harmonic components progressively reflect shorter time domains, as the current response is of a higher frequency. Thus, in the data analysis protocol, the second and higher order harmonic faradaic responses, which are

ideally devoid of a capacitance current, can be parameterised in a Bayesian framework.[8] The equivalent scenario in DC voltammetry would be to analyse data over a range of scan rates and implement "scan rate updating". However, use of this technique requires a series of experiments to be undertaken with an electrode with potentially variable surface states due to intermittent re-polishing of the electrode and there is always significant background charging current especially at high scan rates. In comparison, parameterisation in FTAC voltammetry using a series of harmonics can based on just a single experiment with negligible background capacitance current and progressively enhanced kinetic sensitivity in the higher order harmonics. Figure 1g shows the high sensitivity of 6^{th} harmonic of the FTAC voltammetry to specified regimes of experimental conditions and electron transfer kinetics summarised in Figure 1g. In particular, a significant change in the current magnitude is associated with the 6^{th} harmonic when k^0 increases from 0.07 to 0.28 cm s^{-1}, until the reversible limit for this harmonic is approached. In contrast, the corresponding total current data, which is dominated by the fundamental harmonic component is essentially indistinguishable from the reversible one in this same kinetic regime. The kinetic sensitivity is of course also a function of frequency.

A subtle but important issue that has generally been avoided in multi-parameter estimations based on comparisons of simulated and experimental voltammetric data is that values reported are likely to be a function of the method of data analysis employed.[27] Clearly, differences in outcomes of parameter values derived from manually implemented heuristic and computer supported data optimisation based approaches almost inevitably will occur. However, parameter estimates can also be a function of the algorithm used for of computationally based data optimisation. This often neglected aspect of voltammetric data analysis is specifically addressed in this paper in the context of the large amplitude AC method, but is applicable to all forms of the technique. In practice, when an AC data set is collected and mathematically described models are selected for simulations, there are many ways of undertaking comparisons with experimental data. In this study, we have compared the outcome of the estimation of up to seven parameters from ten AC voltammetric data sets in conjunction with Bayesian inference. The MCMC method is used to calculate the posterior probability for "noisy" synthetic data and experimental data for the $[Fe(CN)_6]^{3-/4-}$ process in aqueous 3.0 M KCl electrolyte at a gold electrode using total (AC plus DC) current,[15] the power spectrum and harmonic envelope based objective functions.The AC experimental conditions used to determine the

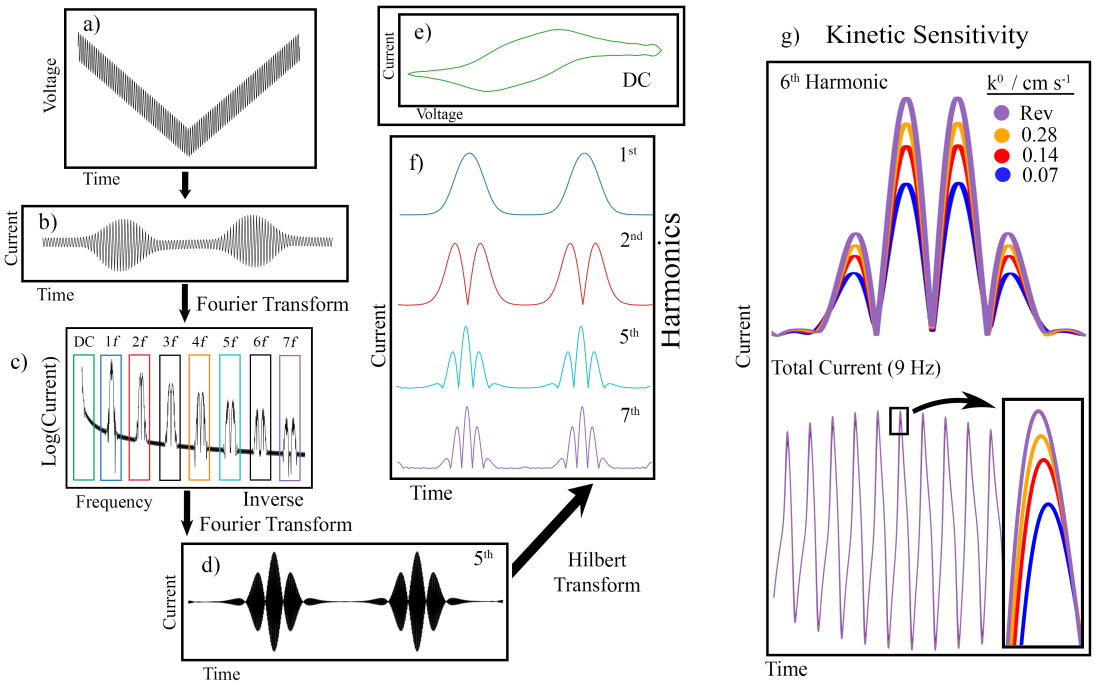

Figure 1: Diagram showing the procedure used for resolving the aperiodic DC and AC harmonic components from FTAC voltammetric experimental data (with set amplitude (ΔE) and frequency (f)). a) applied sinusoidal waveform. b) resultant total current, c) power spectrum with rectangular windowing used to define regions used to resolve individual components by inverse Fourier transformation, d) resultant fifth harmonic, e) aperiodic DC component and f) envelope version of AC harmonics where the colour of the harmonic corresponds to the frequency region they are derived from in the power spectrum. g) The effect of the electron transfer rate (k^0) on the total current and the kinetically more sensitive 6^{th} harmonic, for k^0 close to the reversible limit and the reversible case (Rev). Simulation parameters beside k^0 are sine wave amplitude of 80 mV s^{-1}, $f = 9.0$ Hz, $D = 5.5 \times 10^{-6}$ cm^2 s^{-1}, $R_u = 0$ Ω, $C = 1.0$ mM, $\alpha = 0.5$, $E^0 = 0$ mV and T = 295 K.

electrode kinetics were deliberately chosen so that the $[\mathrm{Fe(CN)_6}]^{3-/4-}$ process is close to reversible to make this a stiff problem with high prospects for reporting data analysis dependent electrode kinetics.

A major issue in data analysis that needs to be understood is that the models used in simulations to mimic both experimental faradaic and double layer capacitance current-potential behaviour are only approximations. That is, the models themselves are invariably imperfect in describing the physical processes relevant to the problem. Consequently, variation in the outcome of modelling arise with different methods of data analysis. Accordingly, which AC data format is used, which simulation-experiment comparison technique is used and which Bayesian inference sampler is employed are therefore all critical in the parameter estimation outcome when fitting simulated to experimental data.

2 Experimental

DC and AC voltammmetric studies were undertaken at 21 ± 1 °C in an aqueous (MilliQ water purification system) solutions containing 1.0 mM $K_3[Fe(CN)_6]$ and 3.0 M KCl as the supporting electrolyte. The solutions were de-aerated by bubbling with N_2 for at least 5 minutes prior to measurements with a flow of N_2 maintained above the solutions during experiments. $K_3[Fe(CN)_6]$ was obtained from (Sigma-Aldrich) and recrystallised from methanol. KCl was sourced from Merck (Analytical Grade 99%). A conventional three electrode electrochemical cell was used with a gold macrodisc working electrode having nominal diameter of 2.0 mm, a Ag/AgCl (3.0 M KCl) reference electrode (CH Instruments) and a platinum wire counter electrode. The procedure used to clean the gold electrode prior to each experiment was to polish with an aqueous 0.3 micron aqueous alumina slurry, rinse surface of the electrode with high purity water, lightly sonicate for a few seconds finally rinse with high purity water, acetone and high purity water in a three step process, then dry thoroughly with pressurised N_2 gas. The DC voltammetric measurements employed a CHI 760E electrochemical workstation (CH Instruments). FTAC voltammetric experiments where conducted with custom designed instrumentation [11,28] using a sinusoidal waveform having an amplitude of 80 mV and frequency of 9.02 Hz superimposed onto a DC ramped voltage having a scan rate of 89.41 $\mathrm{mV\,s^{-1}}$.

The gold working electrode surface area was calibrated as 3.36×10^{-2} $\mathrm{cm^2}$ by reference of the DC peak current obtained for the one-electron reversible oxidation of 1.0 mM $[Fe(C_5H_5)_2]$ (Fluka) in acetonitrile (100 mM $(BuN)_4PF_6$) to the Randles-Sevcik equation. A literature value of the diffusion coefficient of 2.4×10^{-5} $\mathrm{cm^2\,s^{-1}}$ [29] was used in this electrode area calibration exercise.

3 Generating Synthetic Data

Synthetic AC voltammetric data for a quasi-reversible process based on the Butler-Volmer of electron transfer were generated using MECSim [7] software with a sine wave amplitude of 80 mV, frequency of 9.02 Hz and a ramped DC potential having a scan rate of 100 $\mathrm{mV\,s^{-1}}$. The ten synthetic AC experiments had their E^0, R_u, D, c_0, k^0 and α values randomly generated within a specified range from a Gaussian distribution with the true calculated mean and standard deviation of the ten synthetic AC experiments shown in Table

1. The ten data sets therefore represent the system reproducibility with realistic experiment-to-experiment variability which can be seen by visual inspection of AC voltammograms contained in Figure S1 in the Supporting Information. In this case the k^0 value in the vicinity of 5.02×10^{-2} cm s^{-1} which is well removed from the reversible limit so represents a relatively straightforward data analysis exercise. The synthetic data was generated assuming no correlation between parameters in the Gaussian distribution. To even more realistically mimic experimental data, Gaussian noise was added to the current with a magnitude of one percent of the maximum absolute current for each of the ten synthetic data sets. The harmonics of the ten synthetically generated experiments are provided in Figure S1. The noise in the background the 6^{th} and 7^{th} harmonic is predominantly due to the pseudo random noise added to the synthetic data.

Parameter	Gaussian Distribution (Mean±Standard deviation)
D / cm^2 s^{-1}	$(5.50 \pm 0.02) \times 10^{-6}$
E^0 / mV	-0.37 ± 1.26
k^0 / cm s^{-1}	$(5.02 \pm 0.11) \times 10^{-2}$
α	0.540±0.002
R_u / Ω	52.1 ± 7.6
C_{dl} / µF cm^{-2}	38.9 ± 5.4
σ_{noise} / nA	764 ± 16

Table 1: The mean and standard deviation of the parameter values used to simulate the ten synthetic AC voltammetric data sets. The parameters are Gaussianly distributed with means and standard deviations shown.

4 Data Analysis Program Details

The code developed for the analysis of the large amplitude AC voltammetric data is open source and can be found on GitHub. The code was designed and written to be used inside a singularity container [30] for portability and use on parallel computing systems. The MECSim software used to simulate the AC voltammetry is written in Fortran 77 code and is wrapped in a Numpy [31] F2PY wrapper which can call MECSim as a subroutine to provided high computational efficiency and for supercomputer use. A executable version of the code for AC voltammetry analysis is available on GitHub as BIOMEC for use. Code documentation and a tutorial can be found on the above mentioned link. All calculations were undertaken on an Ubuntu operating system with software run on an Intel generation 8 CPU with the two CPUs used having clock speeds of 1.8 GHz and 3.2 GHz. Additional supporting code can be found in the previously mentioned GitHub repository.

5 Theory

5.1 Modelling

Simulations of large amplitude AC voltammetry were undertaken with the Monash Electrochemistry Simulator (MECSim) software package.[7] For mathematical and computational details the reader is referred to the paper by Kennedy et al.[7] Simulations of the faradaic current for a quasi-reversible one-electron transfer process (Eq.(1)) as a function of applied potential ($E(t_i)$) are based on the Butler-Volmer equation[3] (see Eq.(2)), where $E(t_i)$ is the time dependent applied potential and t_i represents the time corresponding to point i in a discrete time domain. Mass transport was modelled by planar diffusion (Eq.(3)), $C_A(0,t_i)$ and $C_B(0,t_i)$ are the surface concentrations of A and B respectively and F is Faraday's constant. The faradaic current is then added to the double layer current to provide the overall current seen in Eq.(4).

$$\mathrm{A} \rightleftharpoons \mathrm{B} + \mathrm{e}^- \quad (E^o, k^o, \alpha) \tag{1}$$

$$\begin{aligned} I_f(t_i) = FA_{we}k^o \Bigg[C_A(0,t_i)\ \exp\left((1-\alpha)\frac{F}{RT}(E(t_i) - I(t_i)R_u - E^o)\right) \\ - C_B(0,t_i)\ \exp\left(-\alpha\frac{F}{RT}(E(t_i) - I(t_i)R_u - E^o)\right)\Bigg] \end{aligned} \tag{2}$$

$$\frac{\partial C}{\partial t} = D\frac{\partial^2 C}{\partial x^2} \tag{3}$$

$$I(t_i) = I_f(t_i) + I_{Cdl}(t_i) \tag{4}$$

In DC cyclic voltammetry, the potential was varied from an initial value to a switching potential and back to the initial value as shown in Eq.(5) where the sweep direction is reversed at half the experimental time where full completion time is denoted as ($\hat{T}$). In AC voltammetry, the sinusoidal signal is superimposed on top of the DC signal as in Eq.(6). The AC signal is represented by Eq.(7) where ΔE is the potential

amplitude and f is the applied frequency.

$$E_{DC}(t_i) = \begin{cases} E_{start} + \nu t_i, & \text{if } t_i \leq \hat{T}/2 \\ E_{switch} - \nu t_i, & \text{if } \hat{T}/2 < t_i \leq \hat{T} \end{cases} \tag{5}$$

$$E(t_i) = E_{DC}(t_i) + E_{AC}(t_i) \tag{6}$$

$$E_{AC}(t_i) = \Delta E \ \sin(2\pi f t_i) \tag{7}$$

The simulations also accommodate the contribution of the double layer charging current (I_{Cdl}). Since the background current is dependent on the applied potential, $C_{dl}(t_i)$ was described via use of an empirical nonlinear capacitor model[32] and obtained by fitting the fundamental harmonic background current to the polynomial function described in Eq.(8). The double layer charging current is calculated using Eq.(9). The simulated current is the sum of Eq.(2) and Eq.(9). For Bayesian inference calculations, the parameter S in Eq.(9) is introduced as a scalar to accommodate experiment to experiment variability in capacitance current. S values are normally very closely to one.

$$C_{dl}(t_i) = c_0 + c_1 E_{DC}(t_i) + c_2 E_{DC}(t_i)^2 + c_3 E_{DC}(t_i)^3 + c_4 E_{DC}(t_i)^4 \tag{8}$$

$$I_{Cdl}(t_i) = S\left[C_{dl}(t_i)\frac{\partial E(t_i)}{\partial t_i} - R_u \frac{\partial I(t_i)}{\partial t_i} + (E(t_i) - I(t_i)R_u)\frac{\partial C_{dl}(t_i)}{\partial t_i}\right] \tag{9}$$

The AC current data in each experiment was assumed to contain Gaussian distributed noise whose variance in some cases was treated as a parameter to be estimated in solving the inverse problem. A list of parameters fitted in this study is provided in Table 2.

Parameter	Description
D / $\mathrm{cm^2\,s^{-1}}$	Diffusion coefficients assuming $D_A = D_B$
R_u / Ω	Uncompensated resistance
k^0 / $\mathrm{cm\,s^{-1}}$	Charge transfer rate constant
E^0 / V	Reversible potential
α	Charge transfer coefficient
$C_{dl}(t_i)$ / $\mathrm{F\,cm^{-2}}$	Potential dependent double layer capacitance
S	Scalar to adjust double layer capacitance current
σ_{noise} / A	Noise in current

Table 2: Parameters used to fit the experimental and synthetic AC voltammetric data.

5.2 Bayesian Inference

Bayesian inference is a statistical method of analysis for experimental data (I^{Exp}) that samples the posterior distribution ($P(\theta|I^{Exp})$) of a parameter set denoted as θ using Bayes' theorem shown in Eq.(10). An example parameter set used to simulate a quasi-reversible heterogeneous one electron process is shown in Eq.(11). The Bayesian approach allows the best fit between experimental and simulated data to be achieved as well as provides a probability distribution for a parameter set derived from a comparison of simulated and experimental data.

$$P(\theta|I^{Exp}) = \frac{P(I^{Exp}|\theta)P(\theta)}{P(I^{Exp})} \tag{10}$$

$$\theta = \{D, R_u, E^0, k^0, \alpha, C_{dl}, \sigma_{noise}\} \tag{11}$$

In Bayes' theorem, $P(\theta)$ is the prior distribution of θ, which represents the prior knowledge of the parameter set that is being fitted. For Bayesian inference calculations the prior is assumed to be uniformly distributed over possible values of the parameter. The distribution $P(\theta|I^{Exp})$ is the probability density or posterior distribution of the parameters for the particular parameterised model in comparison to experimental data, whereas, $P(I^{Exp})$ is the marginal likelihood term or the probability of the experimental data. The posterior distribution can be calculated from experimental data based on a noise model on the basis that the posterior distribution of each parameter is a Gaussian distribution around a mean of the best fit and standard deviation. The noise model of the experimental currents assumes that the T_{max} data points are independent

measurements and are Gaussianly distributed around a mean current, where the standard deviation of the experimental current is then dependant on the relevant noise parameter (σ) present in the likelihood function shown in Eq.(12).

$$\begin{aligned} L(\theta|I^{Exp}) &= \prod_{i=1}^{T_{max}} P(I^{Exp}(t_i)|\theta) = \prod_{i=1}^{T_{max}} \mathcal{N}(I^{Exp}(t_i)|I^{Sim}(t_i,\theta),\sigma^2) \\ &= \prod_{i=1}^{T_{max}} \frac{1}{\sqrt{2\pi\sigma^2}} \exp\left(-\frac{(I^{Exp}(t_i)-I^{Sim}(t_i,\theta))^2}{2\sigma^2}\right) \end{aligned} \tag{12}$$

$$P(\theta|I^{Exp}) \propto P(I^{Exp}|\theta)P(\theta) = L(\theta|I^{Exp})P(\theta) \tag{13}$$

Finally, $P(I^{Exp}|\theta)$ is the evidence term and represents the probability of the experimental data given the parameter set and is used to update the prior in Bayes' theorem. In Bayesian inference, $P(I^{Exp}|\theta)$ is substituted by the likelihood function ($L(\theta|I^{Exp})$) when incorporating σ_{noise} into the inference problem when comparing the experimental to simulated data. This method is related to Bayes's theorem via Eq.(13), and has the marginal likelihood ($P(I^{Exp})$) removed. Since the likelihoods calculated using Eq.(12) are extremely small for the large number of samples used, a rearranged log-likelihood is incorporated for undertaking the inference calculation via use of Eq.(14) in order to sample the posterior distributions of the parameters involved in the simulation. A more detailed explanation of the statistical modelling used in this work is contained in the paper describing the application to total current AC voltammetry by Gavaghan et al.[15]

$$l(\theta|I^{Exp}) = -\frac{T_{max}}{2} ln(2\pi\sigma^2) - \frac{1}{2\sigma^2} \sum_{i=1}^{T_{max}} \left(I^{Exp} - I^{Sim}(t_i,\theta)\right)^2 \tag{14}$$

To sample the posterior probability itself, the MCMC method or more specifically in this work, the Adaptive Covarience MCMC method[33–35] is used. The MCMC method is a complex method of sampling the posterior which iteratively trials new simulations to compare to experimental data. The concept is to construct a chain of accepted parameter sets with distributions that approximate the posterior distribution. The initial starting point for the MCMC method is an optimum that has been identified via an optimisation algorithm, which in this study is the stochastic Covariance Matrix Adaptation Evolution Strategy (CMA-ES)

developed by Hansen.[36]

The MCMC calculations utilised four chains for multivariate objective functions as explained below. Each chain has a length of 10,000 iterations. Thus, the total chain length required 40,000 simulations, with the Gelman-Rubin statistic being used to test convergence of chains,[17] which were also employed to confirm that a unimodal posterior distribution is present. A single chain length of 10,000 was used for the total current based objective functions, shown in Eq.(14). Once the MCMC calculations were finished, the first 25% of calculations were "thrown away" or removed from the inferred distribution as they represent the "burn in" period. Depending on the speed of the computer used, four to eight hours were required to complete the MCMC calculations with each individual simulation taking one to two seconds on the hardware reported in Section 4.

6 Overview of Data Analysis Methods

Optimisation to estimate parameters present in a model is a mathematical process of finding the local minimum/maximum of a specified objective function ($Loss(\theta)$) derived by comparison of experimental and theoretical data. In dynamic voltammetry, the comparison is generally between experimental and simulated current data obtained as a function of potential.[7,11,18] In DC cyclic voltammetry the optimisations technique compares the singular univariate DC current to the simulated current as a function of the time dependent potential.[37] In contrast, large amplitude AC voltammetry possesses a range of data formats or structures available for comparing the experimental and simulated data. Data optimisation for a simple one electron quasi-reversible process based on analysis of the total (DC plus AC) current (Figure 1a and harmonic envelope content (1f) formats obtained by Fourier transformation have been investigated by Morris et al.[27] using the Nimrod toolkit[38] to compare experimental and simulated AC voltammetric data. Use of the Nimrod toolkit also has been extended to other mechanisms with caution advised in multi parameter parameterisation to the significant possibility of over fitting the simulation.[39–42] The present work expands the range of AC data formats that can be used to present experimental data and subjected to data optimisation analysis. The use of Bayesian framework provides access to uncertainties in parameter values reported. Results reveal that estimates of parameter values and uncertainties can be dependent on the objective function used in the data

analysis exercise.

Comparison methods are represented mathematically by objective functions, which are generally denoted as $Loss(\theta)$ in this paper. The investigation to determine which objective function to recommend when comparing experimental and simulated AC voltammetric data considered in two categories; the univariate time series case, where a singular time series is compared and the multivariate case where multiple time series are compared using multiple harmonic envelope forms of data. The data optimisation algorithm employed is CMA-ES[36] and the Adaptive Covariance MCMC method is employed for Bayesian inference calculations.[33]

6.1 Univariate Objective Functions

6.1.1 Total Current Difference Squared

In univariate time series methods, the Loss function provides a comparison of a singular series of data either in the time domain or frequency domain. The most direct method of comparison of experimental and simulated data in large amplitude AC voltammetry is achieved via use of the total (AC plus DC) current difference squared (TCDS) objective function given in Eq.(15) and used in previous studies.[27,42]

$$Loss(\theta) = \sum_{i=1}^{T_{max}} \left(I^{Exp}(t_i) - I^{Sim}(t_i, \theta) \right)^2 \tag{15}$$

6.1.2 Maximum Likelihood Estimated Total Current Difference Squared

Since the optimisation algorithm fits to experimental data will vary around a mean value to an extent governed by the degree of noise (σ), maximum likelihood estimation methods based on the log-likelihood function shown in Eq.(14) can be used for parameterisation. In the application of the CMA-ES algorithm, these log-likelihood functions are referred to as the $Loss(\theta)$ objective functions and the absolute value is used for minimisation. This maximum likelihood estimated total current difference squared (MLE-TCDS) value is used as the objective function for optimisation assuming a variable degree of noise (σ) and can be used in Bayesian inference as well as data optimisation calculations. In this study, the Probabilistic Inference on Noisy Time Series (PINTS)[43] Python library is used to calculate the probability distribution and optimisation of Eq.(14).

PINTS has been used previously to fit synthetic and experimental total current AC voltammetric data.[15,16,44–46] However, a major advantage of large amplitude AC voltammetry, not available in the total current method, is access to resolved harmonics at integer multiples of the frequency of the applied sine wave. These harmonics provide variable levels of sensitivity to some of the parameters of interest in this study.[47] For example, higher order AC harmonics are more sensitive to the impact of electrode kinetics and R_u, but very insensitive to background charging current. As such, the data optimisation methods applied to FTAC voltammetry can take advantage of the harmonic dependent information in fitting the data which can be beneficial in enhancing the fidelity of parameter identification.

6.1.3 Frequency Domain

In FTAC voltammetry,and as shown in Figure 1, the AC harmonics and aperiodic DC component are resolved in the frequency domain (denoted by (f_i)) by Fourier transformation ($\hat{f}_t$) of the time domain AC current data. The resultant power spectrum provides the current as a function of frequency. Analysis using this form of data is referred to as the frequency domain comparison (FD) and uses both the real ($Re()$) and imaginary components ($Im()$), shown in Eq.(16).

$$\hat{f}_t\big[I(t_i)\big](f_i) = Re\Big(\hat{f}_t[I(t_i)](f_i)\Big) + i\ Im\Big(\hat{f}_t[I(t_i)](f_i)\Big) \tag{16}$$

Data optimisation undertaken with the FTAC voltammetric data format in this study is based on absolute difference squared of the truncated frequencies as in Eq.(17), where the frequency domain has been cut to only include $0 - 40$ Hz, as shown in Eq.(17). As such, in this study when using a frequency of about 9 Hz, data from the first 4 harmonics are used as the magnitudes of the fifth and higher order harmonics is relatively small and particularly with experimental data have poorer signal to noise ratios. Use of the Fourier transform algorithm to obtain a frequency dependant current response ($\hat{f}_t\big[I(t_i)\big](f_i)$) filters out most of the random noise in the experimental data. Random current noise is predominantly at higher frequency than 40 Hz. By removing this higher frequency data and only utilising data at specific frequency regions at integer multiples of the input frequency,[47] σ_{noise} is practically removed from the data. Mains frequency pick up noise at 50 and 100 Hz in Australia with present in Experimental but not synthetic data. The mains

frequency is also removed via the Fourier transform filtering procedure The data also provide frequency dependant phase information which requires careful and often complex correction for instrumentally induced phase shifts. Accordingly, data optimisation using the harmonic current magnitudes, which is devoid of phase information, has been used in the majority of studies based on the resolved harmonic content.

$$Loss(\theta) = \sum_{f_i=0}^{40} \left| \hat{f}_t\big[I^{Exp}(t_i)\big](f_i) - \hat{f}_t\big[I^{Sim}(t,\theta)\big](f_i) \right|^2 \tag{17}$$

6.1.4 Power Spectrum Comparison

When the power spectrum displayed in Figure 1c is used in data optimisation, the current as a function of frequency is displayed in the Euler form Eq.(18) where the current modulus $R(f_i)$ and the argument or phase $\varphi(f_i)$ are separated components.[48] The relationship between $R(f_i)$ and the frequency dependant current (Eq.(16)) can be seen in Eq.(19)

$$\hat{f}_t\big[I(t_i)\big](f_i) = R(f_i)\exp\big(i\varphi(f_i)\big) \tag{18}$$

$$\text{where} \quad R(f_i) = \sqrt{Re\Big(\hat{f}_t\big[I(t_i)\big](f_i)\Big)^2 + Im\Big(\hat{f}_t\big[I(t_i)\big](f_i)\Big)^2} \tag{19}$$

Data analysis based on the power spectrum in Figure 1c uses Log_{10} of the current modulus which provides a format that facilitates analysis of additional higher order harmonics. The objective function referred to as the power spectrum (PS) comparison is the least squares difference shown in Eq.(20). Due to the Log_{10} scale of this function the frequency dependant background differs significantly between simulated and experimental and these regions are excluded. However, the Log_{10} of this function allows higher harmonics excluded above to be included in analysis. Now, up to the 8^{th} harmonic signals are used for comparison around the square window region centred of nf plus or minus half the bandwidth (b_w).

$$Loss(\theta) = \sum_{n=1}^{8} \sum_{f_i=nf-b_w/2}^{nf+b_w/2} \Big(Log_{10}\big(R^{Exp}(f_i)\big) - Log_{10}\big(R^{Sim}(f_i,\theta)\big)\Big)^2 \tag{20}$$

In the power spectrum based data optimisation method, it is important to recognise that phase affects

the optimal solution of the objective function. Phase is the backbone of the closely related technique of electrochemical impedance spectroscopy (EIS).[2] In TCDS based comparison methods, the phase also is important as the fit needs to mimic the relationship between potential and current. FD has a similar requirement. However, the power spectrum comparison is affected by the phase to a lesser extent through the exclusion of the phase dependant term $\exp(i\varphi(f_i))$ shown in Eq.(18) which is ignored in Eq.(20) with only the log current modulus being fitted.

6.2 Multivariate Objective Functions

6.2.1 Harmonic Percentage Method

The effect of phase can be avoided if the harmonic envelope form of data is analysed. This data format can for example be derived via the Hilbert transformation shown in Figure 1f and used as the basis of experiment-simulation comparisons instead of the full harmonic sinusoidal current. The use of the envelope form of harmonic data presentation has been widely used in our laboratories to take advantage of the independence on phase.[11] The simplest multivariate technique is the harmonic percentage difference (HarmPer) objective function shown in Eq.(21). An investigation with this objective function has been conducted by Morris et al.[27] These authors found that optimum parameterisation using a harmonic method of optimisation gave a higher selectivity than the total current methods.[27] In this work, the multivariate harmonic envelopes were compared to the mean of the input data harmonic envelopes ($\mu_h(t_i)$) for each harmonic h and the DC component where h equals zero.

$$Loss(\theta) = \frac{1}{H+1}\sum_{h=0}^{H}\sqrt{\frac{\sum_{i=1}^{T_{max}}(\mu_h^{Exp}(t_i) - I_h^{Sim}(t_i,\theta))^2}{\sum_{i=1}^{T_{max}}\mu_h^{Exp}(t_i)^2}} \tag{21}$$

6.2.2 Maximum Likelihood Estimate Experimental Harmonic Percentage Method

The basis of the maximum likelihood estimate experimental harmonic percentage (MLE-ExpHarmPer) objective function and noise model for Bayesian inference is the harmonic percentage equation (Eq.(21)) used in previous literature.[9,42] The advantage of the harmonic percentage is that it normalises the least squared error present in the harmonics when comparing experimental to simulated FTAC voltammetric data. Eq.(22)

is the percentage difference between $\mu_h(t_i)$ and the simulated current ($I_h^{Sim}(t_i)$) for each harmonic h calculated from FTAC voltammetry simulation. In an abstract sense, Eq.(22) is positive when the simulation harmonic maximum is larger then experimental harmonic maximum, negative when the simulated harmonic maximum is smaller and zero when simulation and experimental harmonic maxima are the same.

$$f_h\Big(I_h^{Sim}(t_i,\theta)\Big) = \pm\sqrt{\frac{\sum_{i=1}^{T_{max}}\big(\mu_h^{Exp}(t_i) - I_h^{Sim}(t_i)\big)^2}{\sum_{i=1}^{T_{max}} I_h^{Exp}(t_i)^2}} \tag{22}$$

When using Eq.(22) as the basis for the noise model across each harmonic it is assumed that the percentage fit of the experimental data is Gaussianlly distributed around the experimental data percentage error calculated, with the 10 replicate synthetic and experimental data shown in Figure S1 and S2 respectively in the Supporting Information.

$$f_h\Big(I_{h,j}^{Exp}(t_i)\Big) \sim \mathcal{N}\Big(f_h\big(I_h^{Sim}(t,\theta)\big),(\sigma_h^{Perr})^2\Big) \tag{23}$$

In Eq.(23), σ_h^{Perr} is calculated from the sample variance ($Var()$) of Eq.(22) for all the experimental data sets (j), shown in Eq.(24). This is assumed to be constant for each harmonic and can be calculated directly from the experimental data. The sample variance is taken as it is assumed that the σ_h^{Perr} is an overestimate of the standard deviation in the noise model. It may be possible to apply inference to calculate all the values of σ_h. However, the constant overestimate directly calculated from experimental data is used for simplicity.

$$(\sigma_h^{Perr})^2 \approx Var\Big(f_h\Big(I_{h,j}^{Exp}(t_i)\Big)\Big) \quad for\ j \in \{1, N_{data}\} \tag{24}$$

For the noise model shown in Eq.(23) the likelihood function shown in Eq.(25) is incorporated in the rewritten Bayes theorem shown in Eq.(26).

$$L\Big(\theta|f_h\big(I_{h,j}^{Exp}(t_i)\big)\Big) = P\Big(f_h\big(I_{h,j}^{Exp}(t_i)\big)|\theta\Big) \tag{25}$$

The prior used in the inference fitting are simple uniform distribution, where values outside the distribution are set to a probability of zero.

$$P\Big(\theta|f_h\big(I_{h,j}^{Exp}(t_i)\big)\Big) \propto P\Big(\theta\Big)L\Big(\theta|f_h\big(I_{h,j}^{Exp}(t_i)\big)\Big) \tag{26}$$

In order to apply Bayesian inference to the harmonic time series it is required that the harmonics are independent sets of data. Simulations undertaken at relatively low DC scan rates such as 100 $\mathrm{mV\,s^{-1}}$ with a large sine wave amplitude greater than 60 mV confirm that the harmonic currents are independent of each other as also found in experimental literature,[49] which is important in considering the likelihood function displayed in Eq.(27). Assuming the independence of the harmonics, the conditional probability density for the whole harmonic percentage trace, given the model parameter set θ, is simply the product of the probability density function for each harmonic (h) of each experiment (j) shown in Eq.(27).

$$L\Big(\theta|f_h\big(I_{h,j}^{Exp}(t_i)\big)\Big) = \prod_{h=0}^{H}\prod_{j=1}^{N_{data}} P(f_h\big(I_{h,j}^{Exp}(t_i)\big)|\theta) \tag{27}$$

It is assumed that the variation of the mean harmonic envelope calculated from the experimental sample leads to a Gaussian distribution in the percentage error with a mean of zero and a standard deviation of σ_h^{Perr}, with the noise model being shown in Gaussian form in Eq.(29).

$$L\Big(\theta|f_h\big(I_{h,j}^{Exp}(t_i)\big)\Big) = \prod_{h=0}^{H}\prod_{j=1}^{N_{data}} \mathcal{N}\Big(f_h\big(I_{h,j}^{Exp}(t_i)\big)\Big|f_h\big(I_h^{Sim}(t,\theta)\big),(\sigma_h^{Perr})^2\Big) \tag{28}$$

$$L\Big(\theta|f_h\big(I_{h,j}^{Exp}(t_i)\big)\Big) = \prod_{h=0}^{H}\prod_{j=1}^{N_{data}} \frac{1}{\sqrt{2\pi(\sigma_h^{Perr})^2}}\ \exp\left(-\frac{\big(\ f_h\big(I_{h,j}^{Exp}(t_i)\big) - f_h\big(I_h^{Sim}(t,\theta)\big)\ \big)^2}{2(\sigma_h^{Perr})^2}\right) \tag{29}$$

Finally, the log-likelihood used in the inference calculations, is presented in Eq.(30).

$$l\Big(\theta|f_h\big(I_{h,j}^{Exp}(t_i)\big)\Big) = \sum_{h=0}^{H}\sum_{j=1}^{N_{data}} -\frac{1}{2}ln(2\pi(\sigma_h^{Perr})^2)\ \ -\frac{\big(\ f_h\big(I_{h,j}^{Exp}(t_i)\big) - f_h\big(t,I_h^{Sim}(t,\theta)\big)\ \big)^2}{2(\sigma_h^{Perr})^2} \tag{30}$$

6.2.3 Harmonic Pointwise Method

The Harmonic Point-wise Comparison (HarmPW) objective function method treats every point in every harmonic current envelope as an independent measurement with $\mu_h^{Iexp}(t_i)$ and sample standard deviation

σ_{h,t_i}^{Iexp} calculated from the repeated experiments. Eq.(31) is then optimised to calculate the log-likelihood of the multivariate comparison.

$$l(\theta|\mu_h^{Exp}) = \sum_{h=0}^{H}\left[-\frac{T_{max}}{2}ln(2\pi) - \sum_{i=1}^{T_{max}}\left(ln(\sigma_h(t_i)) + \frac{1}{2\sigma_h(t_i)^2}\left(\mu_h^{Exp}(t_i) - \mu_h^{Sim}(t,\theta)\right)^2\right)\right] \tag{31}$$

Eq.(31) assumes that every single point for every harmonic is Gaussianly distributed around the calculated harmonic current envelope mean with a calculated standard deviation. The inference is then calculated accordingly.

6.3 Incorporation of Bayesian Inference

The log-likelihood function present in the MLE-TCDS, MLE-ExpHarmPer and HarmPW objective functions can be used in Bayesian inference calculations as they represent a noise model (see section 5.2) to sample the posterior distributions. In the univariate log-likelihood case, Bayesian inference is applied to each independent experimental data set to calculate a posterior for each experiment. All j experimental posterior distributions are then added together (pooled) at the end to calculate the overall parameter uncertainty in the replicate data. This outcome is referred to as pooled MLE-TCDS. In contrast, in multivariate data analysis, inference is applied once to the percentage fit to the μ_h^{Exp} to approximate the overall posterior using a single calculation. In this study, each inference calculation was completed in four to eight hours. However, the pooled MLE-TCDS method takes longer to fit the data sets for the ten experiments since the MCMC method has to be applied to each AC voltammetric experiment individually. Thus, the ten experiments require ten posterior distributions to be computed that have to be pooled before reporting overall posterior distributions.

Objective functions that do not incorporate the log-likelihood term are less readily employed in Bayesian inference calculations. However, the accuracy and precision of all the optimal solutions calculated with CMA-ES are validated below. Differences in data analysis formats are summarised in Figure 2. To implement functions that employ AC harmonics, data are truncated in the time domain to remove ringing introduced at the initial and switching potentials. This noise artefact of the inverse Fourier transform algorithm is explained in more detail by Mashkina et al.[50]

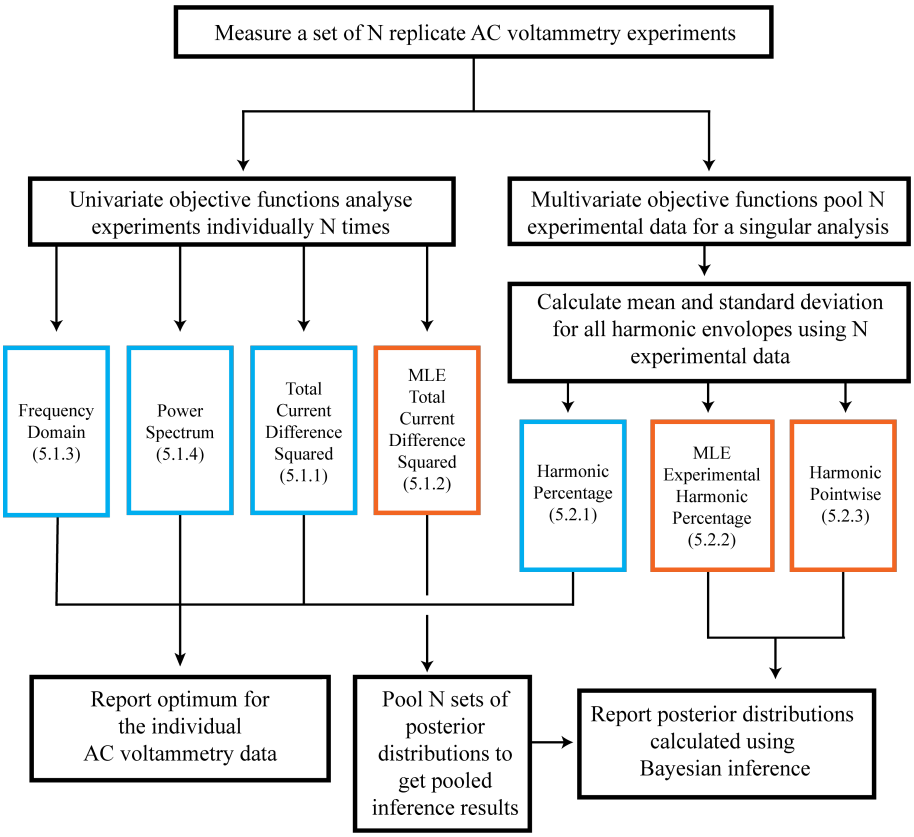

Figure 2: Summary of univariate and multivariate data analysis methods tested on AC voltammetric data in this study. Blue boxes represent an objective function that can only find a optimal solution. Bayesian inference log-likelihood functions are labelled orange.

In summary, the data analysis treatment of the ten repetitive data sets can be categorised into univariate cases where all the data are fitted independently and the multivariate ones where the data mean values are fitted as shown in Figure 2. The optimisation of univariate data objective functions is applied to the total current, frequency domain and the power spectrum data formats (TCDS, FD, PS respectively). Assuming the total current contains Guassianly distributed noise, MLE methods can be applied for optimisation and inference of the objective function (MLE-TCDS). In contrast, the multivariate methods are based on harmonic envelopes as shown in Figure 1f and make use of either the harmonic percentage, an approximated percentage error in the harmonics or the standard deviations in the harmonics themselves to calculate the Bayesian likelihood for the fit (HarmPer, MLE-ExpHarmPer, HarmPW respectively).

For reader's convenience, the acronyms of the objective functions and likelihood functions are listed in Table 3.

Acronym	Meaning
TCDS	Total Current Difference Squared
MLE-TCDS	Maximum Likelihood Estimate - Total Current Difference Squared
FD	Frequency Domain
PS	Power Spectrum
HarmPer	Harmonic Percentage
MLE-ExpHarmPer	Maximum Likelihood Estimate - Experimental Harmonic Percentage
HarmPW	Harmonic Pointwise

Table 3: Summary of the Acronyms used for the objective and likelihood functions.

7 Results and Discussion

The objective functions described in Section 6 were initially tested for optimisation of parameters using 10 similar synthetic AC voltammetric data data sets derived from simulations with known parameter values. Parameters relevant to ten synthetic experiments are summarised in Table 1. Parameterisation of the synthetic data is used to assess the validity of the Bayesian inference methods. Subsequently, the log-likelihood functions were applied to experimental data to test the practical robustness of the Bayesian inference methods. In the FTAC voltammetric harmonic approach, truncation was applied to data such that only 2^{14} data points were used. Thus the $0-1.5$ and $12-13.5$ time regions were removed to avoid fitting to the windowing noise present in these time periods. Accordingly, the truncated 1.5 to 12 seconds data is left for fitting which is the period of time that contains all of the faradaic information, as illustrated in Figure S3.

7.1 Comparison of Data Analysis Methods Using Synthetic Data

The univariate and multivariate objective functions described above were optimised using the CMA-ES algorithm within the same parameter space regions for each of the ten synthetic data sets defined by the Gaussian distributions in Table 1. As the optimisations are fitting a set of simulated data to another set of simulated data, there is no mathematical difference between the physical system and the simulated solution to the partial differential equation, and the parameter values are known. Thus, this form of data, unlike real experimental results can in principle be perfectly matched to the model. [9]

As shown in Figure 3, with the synthetic data, in a broad sense, all data analysis methods provide physically sensible values of recovered parameters, but there is variation at the fine level of detail. Data

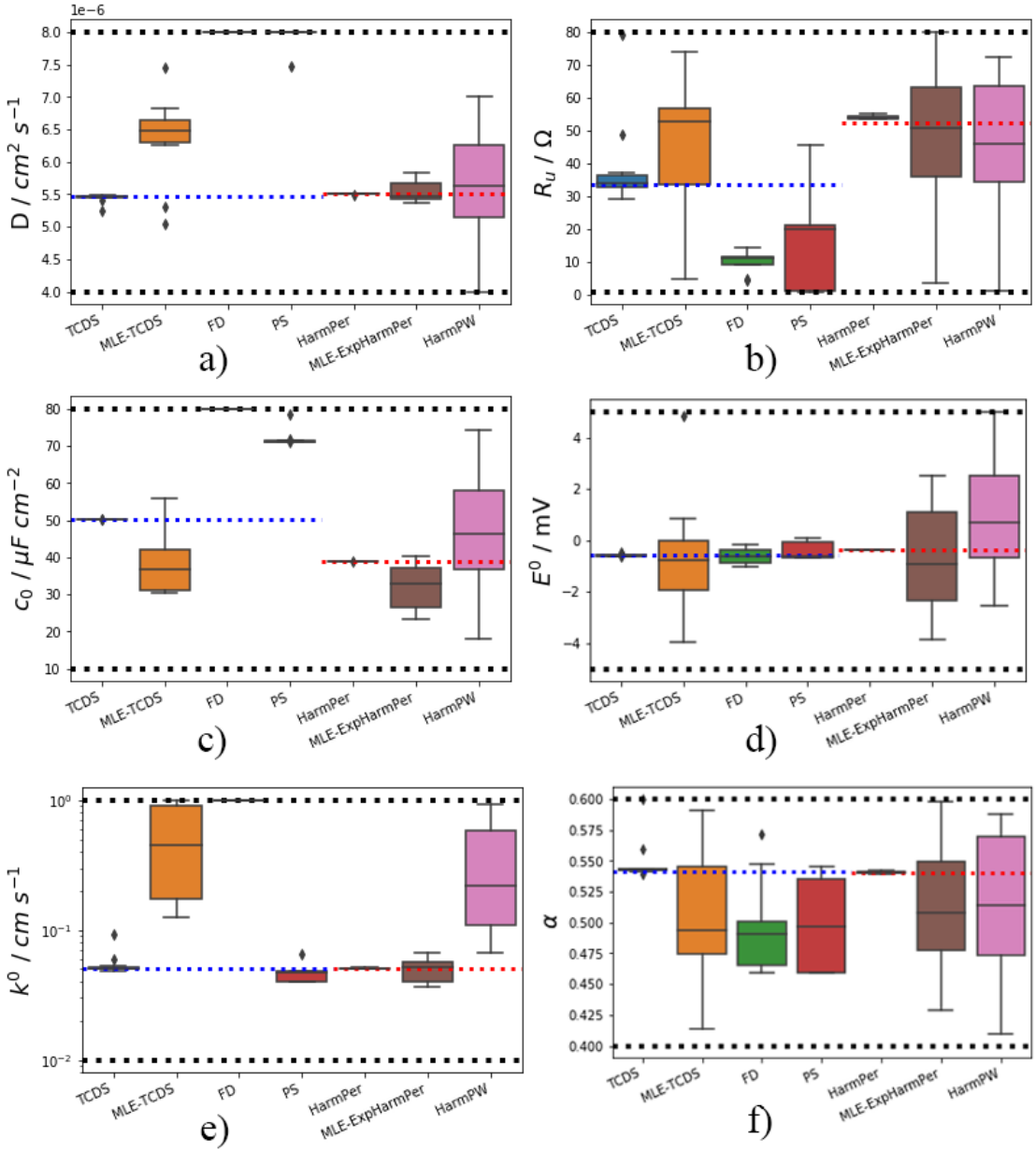

Figure 3: Box plot diagrams of reliability of parameter recovery from synthetic data for large amplitude AC voltammetric optimisation methods considered in this study. Ten optimisations were undertaken within the parameter range of the black dotted lines. The true parameter values for the optimisations are indicated by the blue or red dotted lines. The red dotted lines (−−) represent the mean of the synthetic parameters given in the Table 1. The blue dotted lines (−−) represent the parameters being fit for by the TCDS, MLE-TCDS, FD and PS objective functions. The black dots outside the interquartile ranges of the box plot are labelled outliers.

optimisation based on total current and harmonic percentage has been successfully employed in previous studies.[15,16,44–46] Thus, as expected, the TCDS objective function provides an excellent fit to the synthetic data and excellent recovery for all parameters. On the other hand, the MLE-TCDS objective function slightly

overestimates the faradaic component parameters and underestimates the non-faradaic capacitance ones as shown in Figures 3a, 3c, 3d, even for this simplest possible scenario where the double layer capacitance is simulated and fitted as a potential independent constant (c_0). The poorer parameter recovery for the MLE-TCDS method can be attributed to the requirement for fitting of σ, which is in the range of 0.975% to 1.25% of the maximum current, by the CMA-ES algorithm. The addition of this (seventh) noise parameter adds significant complexity to the optimisation space which leads to a decrease in the accuracy and precision of the parameter recovery.

The MLE-ExpHarmPer method is not as sensitive for the identification of R_u, E^0 and α, as other methods (Figure 3b, d and f respectively). This could be due to the small differences in responses in the harmonic data and the approximation of σ_h making the MLE-ExpHarmPer objective function preform poorly. In comparison to the MLE-TCDS objective function preformed well for parameters that lead to a direct change of the overall current intensity, such as D and k^0, as seen in Figure 3a and e respectively. Again, this is due to the larger effect that these parameters have on harmonic percentage difference. In general, due to reproducibility issues, for optimisation of experimental FTAC voltammetric data it is recommended that the MLE-ExpHarmPer objective function is used with the similar HarmPer objective function to validate the optimised parameter set.

Optimisations based on the FD and PS methods show variable levels of success. The FD method shows significantly lower selectivity in parameter recovery, although recovery for E^0 as for all methods is excellent (Figure 3d), this is due to the important information being densely spaced in small number of data points corresponding to the lower harmonics frequency. The PS method provides excellent precision for recovery of faradaic parameters 3d, 3e, 3f. Thus, use of the PS method may be improved if current scaling parameters such as D are determined separately and hence are not solved as part of the data optimisation exercise.[51,52]

With the multivariate methods, the HarmPer objective function provides a superior level of accuracy and precision with respect to parameter recovery from the synthetic data compared to the MLE-TCDS and the HarmPW ones. The HarmPer and the TCDS method calculated a very similar fit for the parameters and this is due to the comparison to synthetic data. The MLE-ExpHarmPer had enhanced variability in calculation of R_u, E^0 and α, though other parameters were well recovered. This could be due to the

smaller effect that R_u, E^0 and α have on the harmonics and the data being more complex due to the added maximum likelihood estimate process that is occurring. However as the values for σ_h are constant the optimisation should be simpler then the MLE-TCDS method though fits for R_u, E^0 and α are comparable. Of the multivariate methods the HarmPW multivariate method has the lowest recovery accuracy across all parameters in comparison to the harmonic percentage based methods and generally produces a poorer fit of the optimisation functions. This is thought to be due to the existence of small regions of highly over weighted data that occur for the point wise standard deviations. This would cause the optimisation to be chaotic, leading to many best fit local minima.

Due to the fitting of the multivariate methods it is suggested in future work that the HarmPer method is attempted on all FTAC voltammetric experiments to get an approximate point fit of the parameters being optimised. This method of fitting has been used previously by[9,27] and gives the most chemically sensible analysis of the experimental data. Once an approximate value has been calculated using HarmPer objective function the parameters can be identified by the more complex MLE-TCDS or MLE-ExpHarmPer objective functions. As such the output parameter values from MLE-TCDS or MLE-ExpHarmPer functions can be assessed with a decree of confidence that the parameters fit are reasonable and chemically intelligent when compared to the HarmPer objective function output.[53]

7.2 Bayesian Inference Validation

Following the the initial survey to ascertain the level of success with parameter recovery of seven objective functions in terms of stochastic accuracy and precision with respect to the known values present in synthetic data sets, outcomes achieved when the MCMC method is employed in conjunction with the MLE-TCDS and MLE-ExpHarmPer preferred methods using procedures summarised in Figure 2 were examined. The robustness of outcomes were then tested with respect to the fit to each harmonic which allows confirmation, or otherwise, that all aspects of the experiment are satisfactorily accommodated in the modelling. In particular, this allows the significance of any simplifications in the mathematical model to be understood. For example, the impact of the computationally efficient approach calculating the double layer capacitance current for each individual sythetic experiment using the scalar (S) multiple of the fitted capacitance shown in Eq.(8)

can be assessed.

7.2.1 Bayesian Inference Calculations on Synthetic Data

The synthetic AC voltammetric data used with Bayesian inference calculations again employed a k^0 value of of $(5.02 \pm 0.11) \times 10^{-2}$ cm s^{-1} for the quasi-reversible process, along with same parameter values used in the parameter recovery exercise discussed in the above section. In the validation of the Bayesian methodology, after applying the MCMC method to both the MLE-TCDS and the MLE-ExpHarmPer log-likelihoods, the calculated posterior distributions for the six "unknown" parameters in the model as well noise were compared. The outcome is summarised in Figures 4 and 5. The true Gaussian distribution of the parameter values in the synthetic data is provided in Table 1. The MLE-TCDS and the MLE-ExpHarmPer log-likelihoods were implemented by employing identical optimisation and inference algorithms that are available in PINTS. [43]

A significant difference in the inference calculations using MLE-TCDS and MLE-ExpHarmPer log-likelihoods, is that in the former approach, each individual experiment gives an approximate fit of the relationship to the noise via Eq.(14), whereas in the latter one the noise is a function of the reproducibility of the "experiments" as determined via the variability in the percentage fit of the harmonics as approximated from Eq.(24). Accordingly, the harmonic noise is used in the inference equation for the MLE-ExpHarmPer method, whereas the MLE-TCDS approach effectively assumes that the noise is electronic variability present in the measured AC voltammetric current for each individual experiment. As such, the MLE-ExpHarmPer method gives a poorer approximation of the probability distribution when parameter values are distinctly variable in the 10 experimental data sets. This difference can be seen by examining the probability distribution of c_0 and E^0 values displayed in Figure 4c and 4d respectively. Thus, if accurate values are required for the distribution of c_0 and E^0 in replicate experiments, the MLE-TCDS log-likelihood can be used advantageously in fitting large amplitude AC voltammetric data as shown by Gavaghan et al. [15] and Robinson et al. [16]

The MLE-ExpHarmPer log-likelihood gives a good estimate of parameter values when the distribution of the individual posteriors overlap but as expected, is liable to fail in the parameter identification exercise when the true distributions do not overlap. This error can be seen in Figures 4c and 4d by comparing the pooled

MLE-TCDS and the MLE-ExpHarmPer log-likelihoods. Thus, careful interrogation of the data analysis outcome needs to be undertaken when using MLE-ExpHarmPer to establish that distribution overlap occurs in repetitive data sets.

An attractive feature of the MLE-ExpHarmPer technique is that the resolved harmonics offer significantly enhanced electrode kinetic selectivity for estimation of k^0, α [10,54] and advantages in modelling the background current. These advantages are shown more clearly to be significant in discussion presented below based on analysis of real rather than synthetic experimental data. Access to the resolved aperiodic DC component and AC harmonics also facilitates identification of model imperfections preset in real experimental data via detection of apparently harmonic dependent parameter estimates. This may occur for example if the model is based on a simple electron transfer process described by the Butler-Volmer relationship, if the Marcus-Hush model of electron transfer would be more appropriate , if unknown adsorption of oxidised or reduced forms accompanies the electron transfer and is not accommodated in the model [10] or if the double layer capacitance is frequency dependent instead of independent of frequency as assumed in the modelling. [51] Another useful attribute of the harmonic percentage technique is that it is independent of phase [55] when the current envelope data format is used for data analysis. In real experiments, instrumentally induced phase shifts are present. Corrections for this artefact will be imperfect, but of course phase-shifts are not present in the synthetic simulated data. Nevertheless, inference methods using total current data have been developed that successfully incorporate phase estimation as part of the analysis protocol even in high capacitance to faradaic current situations. [45] Thus, in principle, the MLE-TCDS method also could form the basis of an effective black box large amplitude AC voltammetric data optimisation software tool for use with the singular form of experimental data..

Another significant difference between the MLE-TCDS and the MLE-ExpHarmPer log-likelihood is that the former includes a fit for noise (Figure 5). The agreement with the true value of σ achieved with MLE-TCDS with synthetic data is almost perfect. However, this probably is only achieved with synthetic data where there is no correlation of electrochemically related parameters with noise and no modelling error, which is unlikely to be the case with experimental data as shown later. The outcome of correlation of parameters such as k^0 an R_u [2,56] can lead to a better than might otherwise be expected fits in multi-parameter estima-

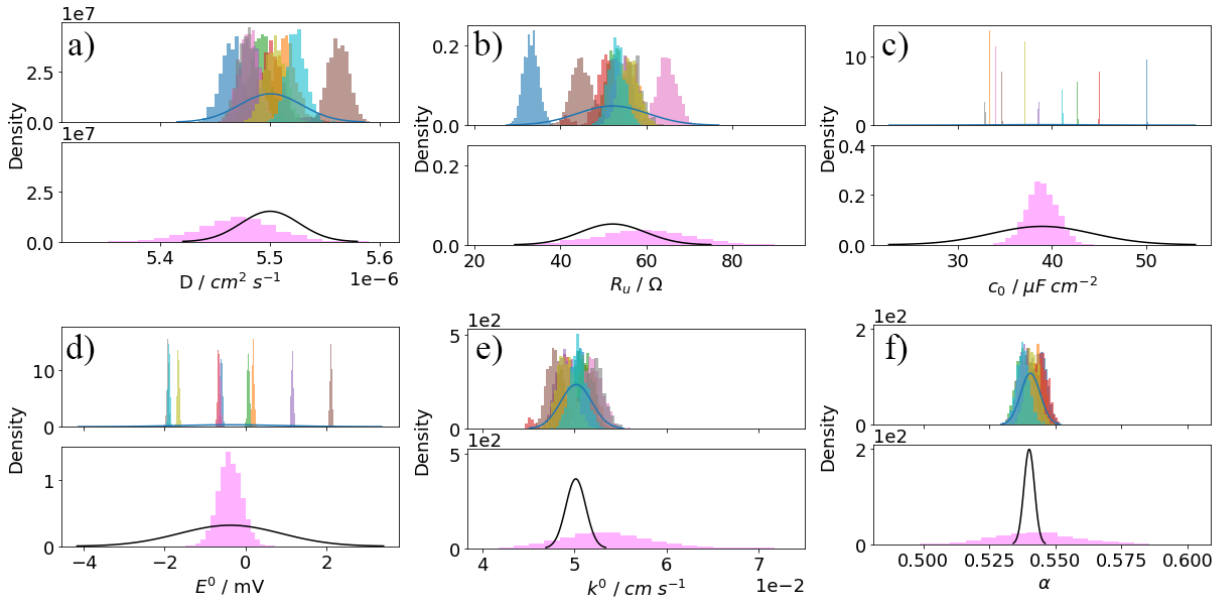

Figure 4: MCMC posterior distributions calculated from synthetic data using the MCMC method with the MLE-ExpHarmPer log-likelihood (bottom magenta histogram) for parameters (a-f) and ten independent MCMC calculations using the MLE-TCDS log-likelihoods for the same parameter sets (top). The blue line (−) are the Gaussian distributions of the pooled MLE-TCDS posterior. The identified parameter sets accuracy is provided in Table 4. The true normal distribution for generating the ten synthetic data points is represented by the black line (−) with parameter values provided in Table 1.

tions. Indeed parameter correlation could be the leading cause of variation between identified and true values obtained when MLE-TCDS and MLE-ExpHarmPer are used with real experimental data. Nevertheless, with the synthetic data, levels of imperfection in the two inference methods are similar.

With synthetic data, the MLE-ExpHarmPer method produces a larger posterior distribution of k^0 and R_u in comparison to the MLE-TCDS one. This is attributable to the sample standard deviation and the sampled synthetic data being generated from a Gaussian distribution (shown in Table 1) assuming no correlation between synthetic parameters. The posterior distribution for the MLE-ExpHarmPer noise model is calculated with a constant value for harmonic noise (σ_h). The competing effects of k^0 and R_u leads to a larger posterior distribution over all the experimental data, which is more apparent in the MLE-ExpHarmPer method due to the data being analysed during a single calculation. The error in k^0 identification is worse for the synthetic data due to the background in the higher harmonics that is a direct response to the pseudo random noise generation of the total current, seen the 6^{th} and 7^{th} in Figure S1.

The identified mean for each independent MLE-TCDS fit and the pooled fit provided the best agreement

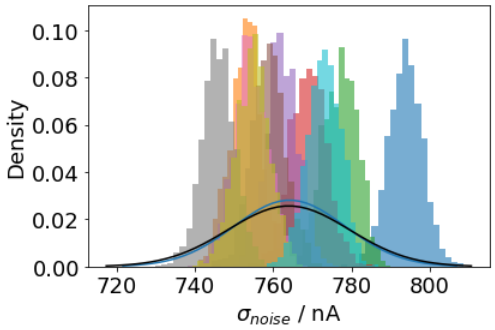

Figure 5: Probability distribution of noise in each of the ten independent synthetic data sets identified using the MLE-TCDS method. The overlaid pooled MLE-TCDS Gaussian distribution (−) and overlaid true (−) distribution from Table 1.

with known values in the parameterisation of the synthetic FTAC voltammetric data sets. In the example studied, the variation in mean is very small for all parameters. The pooled MLE-TCDS inference method accurately identified the distribution of all parameters that do not have overlapping probability distributions. This situation applies to all parameters except for the E^0 and c_0, as shown by reference to Figures 4c and 4d respectively. Thus, the MLE-TCDS approach, while able to identify the mean, was not fully successful in recovering the true probability distribution. In contrast, the Bayesian inference method calculated mean from MLE-ExpHarmPer is able to correctly identify the mean of the generated synthetic data set with less then 8% error as seen in Table 4. Other outcomes of the parameterisation exercise are compared to their true known values along with errors are contained in Table 4. In this Table, the independent MLE-TCDS is the averaged value of each independent fit compared to the simulation, the pooled MLE-TCDS is the calculated mean compared to the mean value given in Table 1 and the MLE-ExpHarmPer outcome is also compared to the same values.

7.2.2 Bayesian Inference Calculations on Experimental Data

When analysing experimental data, unlike with synthetic data, there is no prior knowledge on the level of correctness of the model.[10] Thus, in applying Bayesian inference to parameterise the $[Fe(CN)_6]^{3-/4-}$ process at a gold electrode in aqueous 3.0 M KCl electrolyte, it is assumed as in other related studies[18,54,57,58] that use of the Butler-Volmer theory of electron transfer with mass transport being modelled by planar diffusion will mimic the faradaic current and that the background current can be mimicked by the relationship given in

Table 4: Percentage error of calculated mean to known true value for synthetic data using inference based data analysis method based on Eq.(32). Independent MLE-TCDS mean refers to the mean calculated by each independent MLE-TCDS posterior in comparison to the parameter value used in the simulation. Pooled MLE-TCDS refers to the mean of ten combined MLE-TCDS MCMC posteriors in comparison to the true mean of the synthetic generated data in Table 1. A comparison with MLE-ExpHarmPer mean also is provided.

	Mean Percentage Difference In Parameters						
Bayesian Inference Method	D	R_u	E^0	k^0	α	c_0	σ_{noise}
Independent MLE-TCDS	0.01	-0.16	-4.47	0.07	0.08	0.03	0.1
Pooled MLE-TCDS	0.01	-0.15	1.5	0.05	0.08	0.03	0.09
MLE-ExpHarmPer	-0.05	1.4	4.67	7.02	0.39	0.02	N/A

$$Percentage\ error(\%) = 100 \times \frac{\theta^{\mu}_{calc} - \theta^{\mu}_{known}}{\theta^{\mu}_{known}} \tag{32}$$

Eq.(9). Use of equal diffusion coefficients for oxidised and reduced species also represents an approximation as does neglect of ion-pairing. Thus, there is inevitably model uncertainty and in practice subtle complications such as adsorption of electroactive species will result in a discrepancy between theory and experiment if they are not accommodated in the modelling.[59]

A DC cyclic voltammogram for the reduction of $K_3[Fe(CN)_6]$ is shown in Figure 6a with corresponding AC voltammograms shown in Figure 6b. The reversible potential, approximated from the mid-point potential of the DC cyclic voltammogram and assuming equal diffusion coefficients for oxidised and reduced species, is found to be 366 mV. A D value of $(7.57 \pm 0.08) \times 10^{-6}$ was derived from the Randles-Sevick equation. The peak-to-peak separation value of 63 ± 2 mV, is close to the theoretical value of 57 mV predicted for a reversible process at 20 ± 1 °C.[2] Thus, it is difficult to determine whether this is a quasi-reversible or reversible process by DC cyclic voltammetry at this scan rate since it is challenging to discriminate the effects of uncompensated resistance and slow electron transfer kinetics in this regime.[56] However, the AC voltammetric method is significantly more kinetically sensitive than the DC equivalent one. In principle, data obtained with the AC technique, at least in the FTAC voltammetric form and with a sufficiently high frequency should be sufficiently removed from the reversible limit to allow k^0 and α to be quantified.

In the application of Bayesian inference methods to AC voltammetric data, ten replicate experiments on the $[Fe(CN)_6]^{3-/4-}$ process were undertaken at a gold electrode, using a sine wave having a frequency of 9.02 Hz and an amplitude of 80 mV and with a DC scan rate of 89.41 $mV\,s^{-1}$. In previous studies, it has

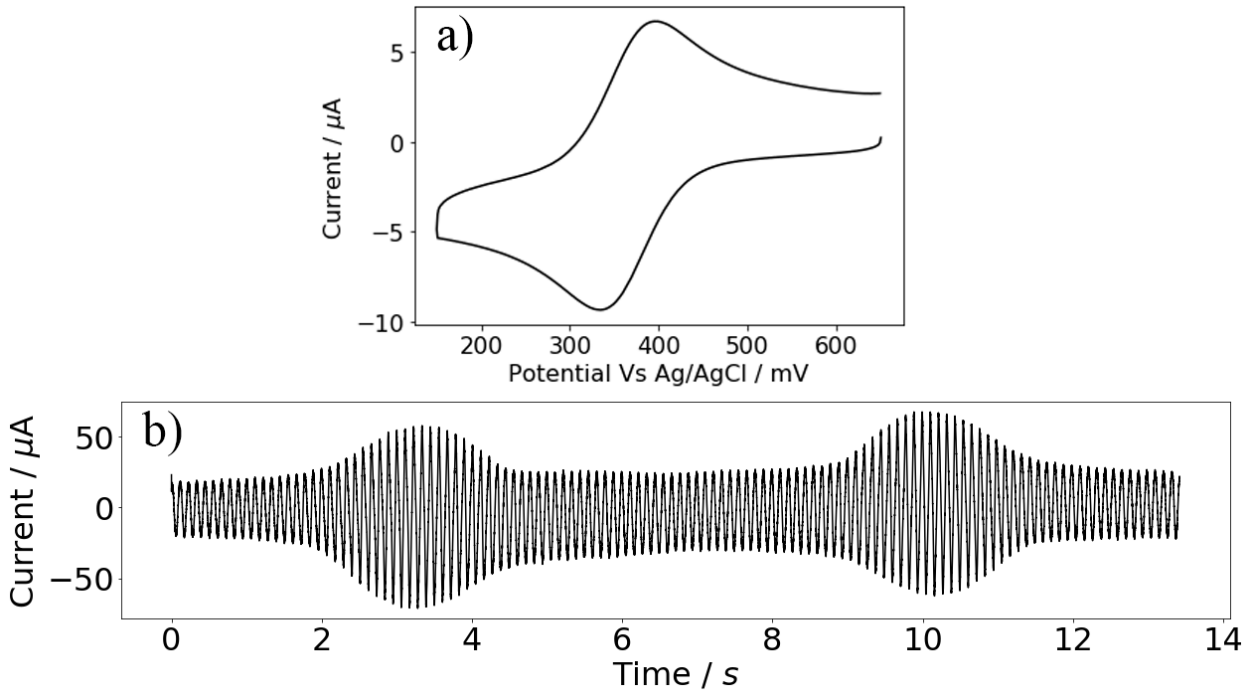

Figure 6: Reduction of 1.0 mM $K_3[Fe(CN)_6]$ at a gold electrode in 3.0 M KCl aqueous electrolyte solution. a) DC cyclic voltammogram obtained with a scan rate of 100 $mV\,s^{-1}$ b) Current-time form of presentation of a large amplitude AC voltammetric experiment using a sine wave with an amplitude of 80 mV amplitude, a frequency of 9.02 Hz and a DC scan rate of 89.41 $mV\,s^{-1}$.

emerged that, even though tedious, initial use of a heuristic approach to estimate parameter values by an experienced electrochemist as a preliminary exercise is valuable in identifying that sufficient sensitivity in the response to parameters present in the model is available, ensure the model is realistic and confirm or otherwise that physically and chemically sensible parameter values have indeed been achieved as the outcome of an automated computerised based parameterisation exercise. The use of heuristic method also enables the parameter search range used in the automated parameterisation process to be restricted, hence save computing time.[27,39,44] Accordingly, parameterisation of the FTAC voltammetric data was first conducted heuristically on one of the ten data sets. The results obtained are summarised in Table 5 and the details of the analysis are given below. The assumption of equal diffusion coefficients for both $[Fe(CN)_6]^{3-}$ and $[Fe(CN)_6]^{4-}$ introduces a systematic error of ≈ 2 mV in E^0 based on literature reported D values of 7.6×10^{-6} $cm^2\,s^{-1}$ and 6.3×10^{-6} $cm^2\,s^{-1}$ for $[Fe(CN)_6]^{3-}$ and $[Fe(CN)_6]^{4-}$, respectively,[2] obtained under similar conditions to those used in this study.

In the application of the very tedious heuristic method, it is almost invariably assumed that all parameters

other than k^0, E^0 and alpha, are either known from the literature or have been independently predetermined. An experienced researcher also knows that that the highest kinetic sensitivity is available in the higher order harmonics. In the present study, visual inspection of data reveals that acceptable signal to noise ratio for the $[Fe(CN)_6]^{3-/4-}$ process is available in the seventh and eighth harmonics for data analysis. Thus in the heuristic method, initial emphasis in evaluation of the electrode kinetics is sensibly placed on obtaining a good fit to these higher order harmonics. When fitting experimental data to simulations, the researcher also can use their experience and discretion to place higher emphasis on specific data regimes (e.g. ignore ringing artefacts in FTAC voltammetry) or ignore areas of data that are considered to be contain irregularities not accommodated by the model.[9] The heuristic method was applied to the experimental data set closest to the mean of the ten data sets analysed computationally. In the heuristic analysis, the literature reported diffusion coefficient value of 7.2×10^{-6} cm^2 s^{-1} was chosen,[16] the resistance value of 15.7 Ω and the value of capacitance was determined from the polynomial fitting of the fundamental harmonic using the region where faradaic response was absent. The value of α was then set to the common value of 0.5 which is common practise for heuristic analysis when a process is close to reversible.[60] Pinning these parameters allows the parameters of interest, specifically k^0 and E^0, to be determined heuristically. When the FTAC voltammetric data was analysed, the reversible potential was first approximated from the midpoint of the harmonics lobes associated with even harmonics or the peak potential associated with the odd harmonics, leaving k^0 the only unknown to be determined. The k^0 is then changed till an acceptable agreement between theory and experiment was achieved based on the visual inspection using the kinetically more sensitive higher harmonics. A k^0 value of 0.21 cm s^{-1} obtained is considerably removed from the reversible limit. This value is close to literature value of 0.25 cm s^{-1} [61] (Row 1 in Table 5) and in the range 0.9-0.23 cm s^{-1} found at Pt electrodes in a aqueous 1 M KCl solution.[62–64]

To assess the capability of the computer based methods in handling large data set with multiple variables all ten replicate AC voltammetric experiments collected for the $[Fe(CN)_6]^{3-/4-}$ process were subjected to simultaneous fitting of all parameters using the MLE-ExpHarmPer and MLE-TCDS Bayesian inference methods, with evaluation of all relevant parameters attempted using the MCMC method based on log-likelihoods. Automated data optimisation described in this study lacks intelligence and will almost always

generate best fit values for all parameters requested. However, the values reported must still be assessed to confirm they are acceptable and may not be if the number of variables estimated is over ambitious under conditions where model uncertainty is present. The best fit values obtained with no parameters pinned are summarised in Table 5. When the MLE-ExpHarmPer Bayesian inference method was used, a D value of $(8.4 \pm 0.1) \times 10^{-6}$ cm^2 s^{-1} was obtained (Row 2 Table 5), which is larger than the value of 7.42×10^{-6} cm^2 s^{-1} reported by Heyrovsky et al.[65] and the value of $(7.57 \pm 0.08) \times 10^{-6}$ obtained from DC voltammetry. The R_u value of 1.24 Ω is significantly smaller than the experimentally determined value of 15.7 Ω while the k^0 value of 0.0875 cm s^{-1} is significantly smaller than the value of 0.21 cm s^{-1} determined heuristically (Row 1, Table 5). This is unsurprising since D, k^0 and R_u are strongly coupled as shown in Figures S4, S5, S7 and S12. Accordingly, underestimation of R_u will result in a underestimation of k^0. Indeed, when the literature reported diffusion coefficient value of 7.2×10^{-6} cm^2 s^{-1} was used, a k^0 value of 0.108 cm s^{-1} obtained was much closer to the literature value (Row 3, Table 5). With the MLE-ExpHarmPer method, an α value of 0.684 was obtained. However, sensitivity to this parameter is poor when the process is close to reversible. E^0 value of 359.7 mV is in excellent agreement with that obtained heuristically. The estimation of this parameter is robust in all data analysis exercises undertaken in this study.

Based on learning gained from the heuristic data analysis, the above outcome suggests that pinning of parameters whose values are well established from independent experiments is warranted. This approach will still provide access to some parameters along with highly important statistical information not accessible form the heuristic examination of just a single data set. When MLE-ExpHarmPer was applied to analyze the same ten FTAC voltammetric data sets with E^0 and k^0 as the only unknown parameters, a k^0 value of 0.140 ± 0.006 cm s^{-1} obtained is close to but certainly not identical to that obtained heuristically (Row 4 in Table 5). The slight discrepancy between this and the heuristically determined values is not surprising since the computer algorithm treats all data points equally unlike an experimenter who may bias the outcome either inadvertently or deliberately, based on experience. The value of k^0 estimated approaches the reversible limit. Computationally supported data analysis therefore was also undertaken using the MLE-ExpHarmPer method assuming the process to be reversible rather than quasi-reversible (Row 5, Table 5). The reversible model, which obeys the Nernst rather than Butler-Volmer relationship, is devoid of k^0 and alpha which

accordingly no longer need to be estimated. For the reversible model analysis, D, k^0, and α are pinned. As such, the best fit to the reversible model is now excellent with a 87.2% fit, but achieved with an R_u value of 79.8 Ω which clearly is an overestimate. In other words, the $[Fe(CN)_6]^{3-/4-}$ process does not provide an acceptable fit to the reversible model under the FTAC voltammetric conditions.

The total current data were also analysed first by the heuristic method. An experienced experimenter would consider the $[Fe(CN)_6]^{3-/4-}$ process to be reversible since there is very little difference in the total current when k^0 is above 0.07 $cm\,s^{-1}$. With the MLE-TCDS method and after calculating the posterior probability, while the method estimated the values for E^0, S and σ with high accuracy, no convergence of D and R_u values was achieved when an attempt was made to simultaneously estimate the seven parameters possible with synthetic data (not shown). This is attributed to the low sensitivity as predicted theoretically (Figure 1) on the basis of findings from the heuristic analysis when data are near to the reversible domain. When the literature value of D and experimentally determined R_u value were used, a k^0 value of 0.0665 $cm\,s^{-1}$ was obtained using the pooled MLE-TCDS method (Row 6, Table 5). This value approaches the reversible limit, again consistent with the finding from the heuristic analysis.

The investigation with real experimental data shows the importance of understanding the impact of parameters and their interrelationships when fitting data derived from AC or indeed any form of voltammetry. Thus, with a quasi-reversible model near the reversible limit, low electrode kinetic sensitivity imposes a greater challenge to modelling the kinetically less sensitive MLE-TCDS method than to the higher harmonics in the FTAC voltammetric data format significantly more removed from the reversible limit k^0.[56,60] Visual comparison of the higher harmonic experimental simulation results shown in Figure 8, reveal poorer agreement achieved with the lower k^0 value derived from the MLE-TCDS log-likelihood with the averaged percentage harmonic best fit of 78.3%, seen in Table 5. Thus, as predicted from an initial heuristic evaluation, for processes that approach the reversible limit under experimental conditions employed here are also advantages in utilising automated data optimisation strategies that emphasise the higher order harmonic data in the fitting process. In the case of the $[Fe(CN)_6]^{3-/4-}$ process at a gold electrode with $f = 9.02$ Hz and $\Delta E = 80$ mV, use of fundamental to eighth harmonic using the MLE-ExpHarmPer log-likelihood gives k^0 of 0.140 ± 0.006 $cm\,s^{-1}$. It is also evident from previous experimental and theoretical studies in large

amplitude FTAC voltammetry by Li et al.[51] that the kinetic sensitivity would increase for the MLE-TCDS likelihood if a higher frequency was applied, but with increased difficulties from enhanced complexities in modelling background charging current and iRu drop. Reliance on best outcome in terms of higher least squares fitting values alone is fraught with danger. For example, an excellent harmonics fit with a percentage error of 87.2% was obtained by data fitting using the reversible model which is comparable to that obtained when parameterisation was achieved with the quasi-reversible models. However, with the reversible case presented, the estimated R_u value of $79.8 \pm 1.2\ \Omega$ is unrealistically high for a 3.0 M KCl electrolyte solution.

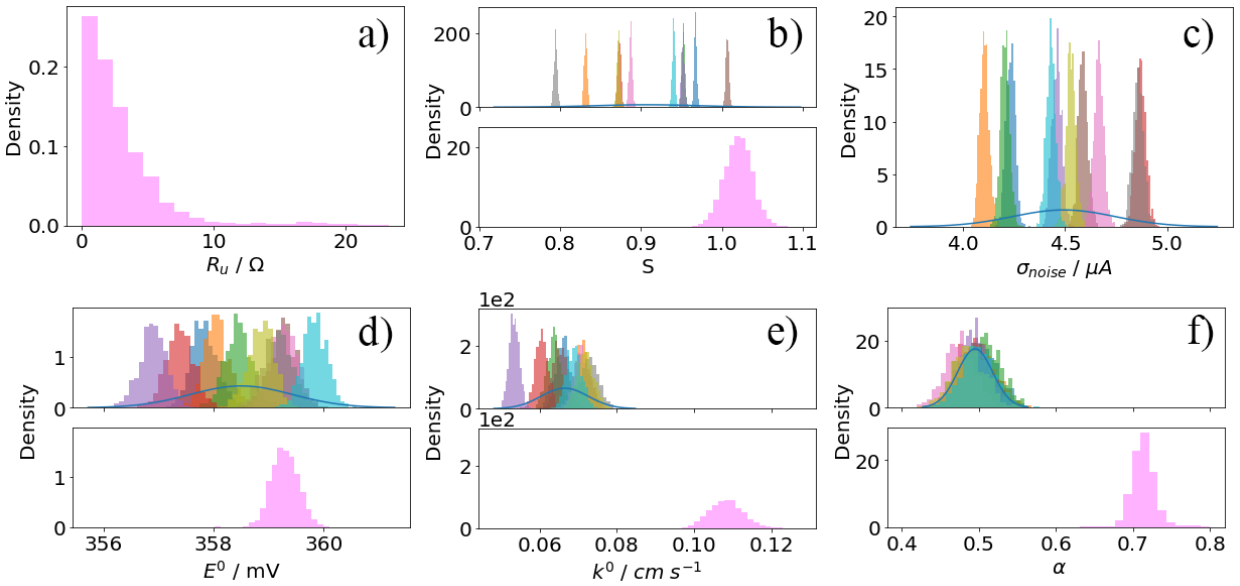

Figure 7: Posterior distributions associated with fitting experimental large amplitude AC voltammetric data for the reduction of 1.0 mM $[Fe(CN)_6]^{3-}$ at a gold electrode in 3.0 M KCl using the MCMC method with MLE-ExpHarmPer log-likelihood (bottom magenta histogram) for parameters a-f and ten independent MLE-TCDS posteriors for parameters c-g (top). The blue line (−) represents the Gaussian distribution of the pooled MLE-TCDS posteriors. Identified parameter values for MLE-ExpHarmPer and pooled MLE-TCDS are provided in Table 5 in rows 3 and 6 respectively. Application of MLE-TCDS with Inference method could not be reliably fit for D and R_u so other parameters were then fitted using experimental or literature values as described in the text. The diffusion coefficient was also set for the MLE-ExpHarmPer for comparisons.

It is also informative to compare the least squares percentage fits achieved with the MCMC, MLE-ExpHarmPer log-likelihood and heuristic fitting methods. All methods as employed, compare the FTAC voltammetric resolved harmonics to various extents of harmonic use and parameter pinning. With the heuristic method, the averaged percentage fit is 88.7% based on use of just one data set. This value is similar to that of 89.4% derived from use of MLE-ExpHarmPer for all ten data sets. Parameters pinned in each

form of data analysis and other details are as described above and summarised in Table 5. In the heuristic method the experimenter has complete freedom to chooses the data analysis protocol which in this case achieved a similar level of fit with the MLE-ExpHarmPer method. Examination of percentage fit of each individual harmonic for the automated methods parameters reveals clearly how the MLE-TCDS method under performed with percentage fits of 95.0% (fundamental harmonic) to 59.5% (eighth harmonic) found for the predicted resolved harmonics. The Total current is dominated by the fundamental harmonic response, with higher order harmonics making a relatively small contribution. In comparison, the MLE-ExpHarmPer log-likelihood emphasises the higher harmonic contributions in the multiple experimental data to give 95.2% to 83.2% for the same harmonics. Overall, differences in the averaged percentage fit are less drastic with values of 77.7% and 89.4% for MLE-TCDS and MLE-ExpHarmPer respectively). A visual comparison of these scenarios is provided in Figure 8.

The MLE-ExpHarmPer noise model uses a noise parameter for the variation between experiments similar to the process used in the MLE-TCDS noise model uses σ to calculate noise in a singular experiment. MLE-ExpHarmPer noise model achieves this by using Eq.(24) to approximate the acceptable variation in the each harmonic envelope percentage fit based on the reproducibility of each of the harmonics, though the use of Bayesian inference on this parameter may be possible. Accordingly, a different weighting is used in each harmonic as seen in the harmonic variation noise calculated via the standard deviation of the percentage errors with values of $\sigma_8^{Perr} = 0.13$ compared to $\sigma_2^{Perr} = 0.025$ and $\sigma_1^{Perr} = 0.045$, with the effect from double layer capacitance being minimal in the experimental data seen in Figure S2. These values of σ_h^{Perr} derived from the ten AC voltammetric experiments, leads automatic fitting method to place a greater emphasis in the lower harmonics, due to the Gaussian distribution σ_h^{Perr} being smaller. When employing the heuristic method, an experienced experimenter has the opportunity to introduce intelligence based thinking into the data analysis. This form of dynamic intelligence is not available in mathematical forms of optimisation or Bayesian inference as implemented in this paper, although biasing the outcome in a preferable direction via smart application of the correct log-likelihood is possible[42] and in the future machine learning could be introduced for this purpose.[53,66] In practice, the heuristic method only provides a single point parameter estimate, does not report the system reproducibility and is so tedious that only about three parameters can

be varied and compared in a series of simulations where comparisons with experimental data are made via visual inspection. Thus, typically all parameters other than E^0, k^0 and α are assumed to be known in the quantification of a quasi-reversible process. Often, α is set to 0.50 for convenience and E^0 is assumed to be the mid point potential derived from a DC cyclic voltammogram to provide even further simplification. In contrast, computer supported Bayesian inference in principle can be used with six or more selected parameters present in the model. Simultaneous multi paramaterisation using Bayesian inference is viable with multiple sets of synthetic data where no model uncertainty is present. In contrast, with real experimental data, uncertainties in modelling both the faradaic and background charging current may need the pinning of variables like the diffusion or uncompensated resistance using reliable values obtained from measurements that are independent of the data optimisation exercise. Without care and using experimenter experience or knowledge gained from an initial heuristic examination of at least one data set it is actually very easy to rapidly get a series of "erroneous" parameter estimates even though "least square type"agreement between experimental and simulated data is excellent.

An important advantage of the MLE-ExpHarmPer log-likelihood method for quantifying the faradaic process by AC voltammetry is that it is possible to use only the second (or third) and higher order harmonics in the data analysis protocol. These data represent almost purely faradaic current and are essentially devoid of background charging current. In contrast, background current can be very significant or even dominant in the total current MLE-TCDS method. Thus, errors in the mathematical model used for the background current are likely to be less severe when fitting is undertaken with the MLE-ExpHarmPer method compared to the MLE-TCDS one. For example, in this study a significant discrepancy in the DC charging current component is evident (as shown in Figure 8a), but agreement of background current is good, but not perfect for the fundamental harmonic for all data analyses based on Bayesian inference with log-likelihoods. Thus, the model for charging current used in the present simulations does not accommodate frequency dispersion present in the experimental double layer charging current data. As the total current is dominated by the DC and fundamental harmonic AC component, Bayesian inference calculations using the MLE-TCDS log-likelihood in circumstances contain some inaccuracy in modelling the capacitance current. In principle, the accuracy of the MLE-TCDS method could be improved if a better capacitance model can be identified.

However, at present, the MLE-ExpHarmPer method is considerably more robust since the second and higher order harmonics used in the MLE-ExpHarmPer method are essentially devoid of background current as shown by inspection of 3^{rd} - 8^{th} harmonics in Figure 8d-i.

Another advantage of the MLE-ExpHarmPer method is that fitting to the multivariate higher order harmonics facilitates uncoupling of the time independent parameters, such as resistance, and the time dependent ones, such as electron transfer kinetics and diffusion.[56] The added robustness of the MLE-ExpHarmPer method also offers advantages when fitting significantly more complex electrochemical processes.[40,41,67] A disadvantage of inference calculations using MLE-ExpHarmPer is that calculating the current envelope and using a Fourier transform to resolve the harmonics makes this approach computationally more expensive than the MLE-TCDS ones. This can be substantial when comparisons of simulated and experimental data are implemented using MCMC methods. However, fortunately with the increase in computation time is only of the order of fractions of a second for every iteration of the simulation with the hardware described in the Experimental Section 4 and the computation time increased, but remains under 6 hours.

In summary, the Bayesian Inference algorithm was validated and tested for the reduction of $[Fe(CN)_6]^{3-}$ at a gold electrode in 3.0 M KCl aqueous electrolyte using the MLE-TCDS and MLE-ExpHarmPer log-likelihoods. For this stiff problem associated with solving the inverse problem for a quasi-reversible, but close to reversible process, access to superior electrode kinetic sensitivity and absence of background current in second and higher order harmonics provides what is believed a superior estimate of k^0 of about 0.14 ± 0.06 $cm\,s^{-1}$ (Table 5, Row 4) and uncertainties when the MLE-ExpHarmPer log-likelihood approach is applied in the Bayesian inference method. The possibility to obtain data analysis method dependent parameter values, as revealed in this study, demonstrates that the implementation of automated parameterisation methods must be undertaken with great caution to ensure accuracy. The preliminary use of heuristic methods, where they can be applied, and checks that chemically and physically sensible parameter values are generated in parameter estimations by automated computationally supported methods is highly recommended. The computationally less expensive MLE-TCDS is ideally suited to data analysis of a quasi-reversible process when the k^0 value measured with an appropriate frequency provides conditions well removed from the reversible limit as shown by Robinson et al.[16] in studies using Bayesian inference applied to the kinetically

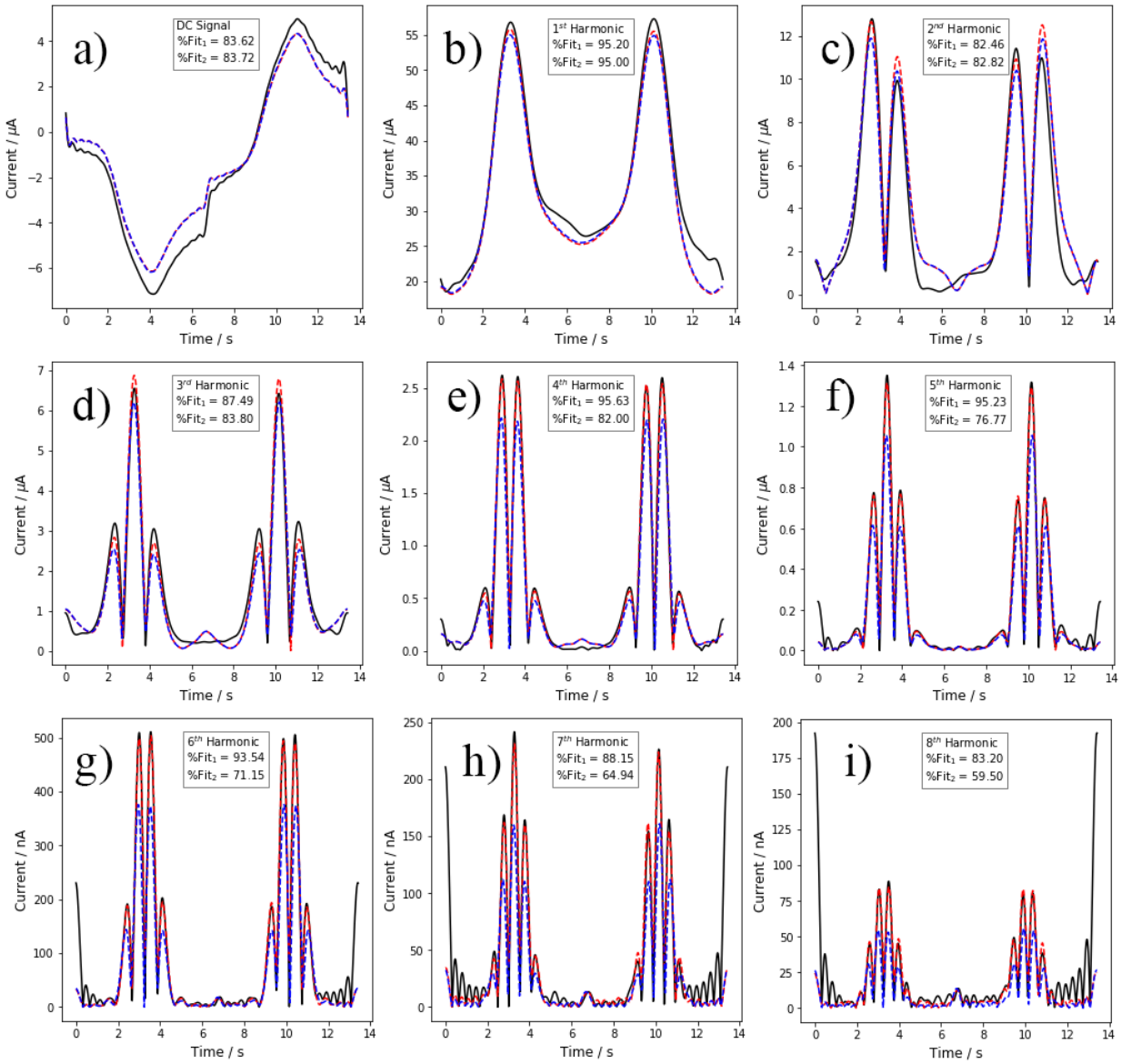

Figure 8: Comparison of simulated and experimental FTAC voltammetric data for the reduction of 1.0 mM $K_3[Fe(CN)_6]$ at a gold working electrode in 3.0 M KCl aqueous electrolyte. Experimental data (——). Simulated data based on mean average for parameters calculated using the MCMC method and MLE-ExpHarmPer log-likelihood (——, Fit_1). Simulated data based on parameters derived from pooled MCMC method using a MLE-TCDS log-likelihood (——, Fit_2). Parameter values for fits Fit_1 and Fit_2 are as summarised in Table 5 in rows 3 and 6 respectively.

slower $[Fe(CN)_6]^{3-}$ etc process at a Glassy Carbon electrode where k^0 is 0.010 ± 0.005 cm s^{-1}. The MLE-TCDS method also could be improved if a model that better mimics the background charging current were available.

Table 5: Calculated posterior distributions for the pooled MLE-TCDS technique and Harmonic Percentage methods derived from a set of ten large amplitude AC voltammetric experiments for the reduction of 1.0 mM $[Fe(CN)_6]^{-3}$ in 3.0 M KCl aqueous electrolyte solution with a a gold electrode. Parameters with no uncertainty provided are set values used for inference calculations or outcomes of a heuristic method which was fitted manually.

Row	Bayesian Inference Method	D / $cm^2\,s^{-1}$	R_u / Ω *	E^0 / mV	k^0 / $cm\,s^{-1}$	α	S	σ_{noise} / μA	Average best fit** / %
1	Heuristic Method	7.2×10^{-6}	15.7	357.1	0.21	0.5	1.0	N/A	88.7
2	MLE-ExpHarmPer	$(8.40 \pm 0.1) \times 10^{-6}$	1.24 ± 1.18	359.7 ± 0.3	$(8.75 \pm 0.33) \times 10^{-2}$	0.684 ± 0.016	0.962 ± 0.02	N/A	89.4
3	MLE-ExpHarmPer Pinned Diffusion	7.2×10^{-6}	2.84 ± 3.00	359.3 ± 0.3	$(1.08 \pm 0.05) \times 10^{-1}$	0.714 ± 0.018	1.02 ± 0.02	N/A	89.4
4	MLE-ExpHarmPer (k^0 and E^0)	7.2×10^{-6}	15.7	357.3 ± 0.2	$(1.40 \pm 0.06) \times 10^{-1}$	0.5	1.0	N/A	88.5
5	MLE-ExpHarmPer, Reversible	7.2×10^{-6}	79.8 ± 1.2	357.3 ± 0.15	1000	0.5	0.99 ± 0.02	N/A	87.2
6	Pooled MLE-TCDS	7.2×10^{-6}	15.7	358.5 ± 0.9	$(6.65 \pm 0.61) \times 10^{-2}$	0.495 ± 0.023	0.908 ± 0.063	4.49 ± 0.25	77.7

* Resistance values are reported as Guassianly distributed but are bounded to be greater then zero. As such, values that are distributed over zero should be considered to be zero plus a standard deviation. ** Calculated based on Eq.(21).

8 Conclusion

Seven objective functions (TCDS, MLE-TCDS, FD, PS, HarmPer, MLE-ExpHarmPer and HarmPW) summarised in Figure 2 encompassing total (AC + DC) current, the power spectrum and the harmonic content available in FTAC voltammetry have been assessed for parameterisation of dynamic electrochemical data obtained from large amplitude AC voltammetry. The methods of data analysis employed are based on automated computer supported optimisation. On the basis of precision, accuracy and robustness, the HarmPer and TCDS objective function gave the best performance as shown in comparison to the synthetic data seen in Figure 3. Prospects for future successful implementation of objective functions based on analysis of power spectra also have been identified.

Data analyses by Bayesian inference methods were applied using the MLE-ExpHarmPer and MLE-TCDS log-likelihood methods. Validation was initially undertaken on ten synthetic AC voltammetric data sets for a quasi-reversible electron process (Butler-Volmer electron transfer model) that were computationally generated using random values of D, R_u, E^0, k^0, α and C_{dl}. Noise was also added. In this data analysis exercise, all parameters could be successfully recovered with all data optimisation methods with ($\theta_{Error} <$ 5%). The MCMC log-likelihoods methods were then applied to the analysis of ten sets of experimental data obtained for the quasi-reversible one-electron $[\mathrm{Fe(CN)}_6]^{3-/4-}$ reduction process at a gold electrode in 3.0 M KCl aqueous electrolyte. One data set was also subjected to classical heuristic data analysis where simulated sets of data and experimental data are compared visually to achieve a good fit, but where data can be deliberately biased using the experience and intelligence of the experimenter. This tedious method of data analysis based on fixed values of D, R_u, α and S provides an estimate of 357.1 mV and 0.21 $\mathrm{cm\,s^{-1}}$ for E^0 (Vs Ag/AgCl in 3M KCl) and k^0 respectively for this experimental setting. While it does not provide access to statistically significant data, the heuristic estimate of parameters does allow the parameter space search to be restricted which is significant in computationally expensive data analysis method. Guidance as to physically and chemically sensible values of parameters that should, but do not always emerge from "non-intelligent" Bayesian inference approaches also is valuable as shown in this study. The close to reversible conditions that prevail when a sine wave of 9.02 Hz and amplitude of 80 mV is used as in this study restrict the use of the MLE-TCDS method to evaluation of E^0, S and σ with high

accuracy. Convergence for D and R_u was not achieved due to the low sensitivity of this method. When D and R_u were pinned, reasonable, but what are assessed as slightly underestimated k^0 values and their uncertainties could be obtained. In contrast, the MLE-ExpHarmPer log-likelihood is weighted towards data obtained for the higher order harmonics that are more sensitive to the electrode kinetics than the total (AC plus DC) current method which is effectively dominated by the longer timescale fundamental harmonic. This provides access to enhanced robustness in calculating the posterior probability of all parameters to be estimated in the simulation of the model and allows uncertainties to be estimated in a Bayesian framework. Nevertheless, ambitious attempts to simultaneously evaluate D, R_u, E^0, k^0, α and C_{dl} that were successful with synthetic data produced parameter dependent degrees of success, with determination of E^0 being most robust. There is no modelled error in synthetic data, but this is significant consideration when parameterising real experimental data. Detailed consideration of correlations of parameters available from Bayesian inference methods and knowledge gained for heuristic analysis facilitated selection of parameters that should be pinned and selection of data regimes providing sensitivity needed for restricted parameter estimation. This led to preferred value of E^0 and k^0 of 357.3 ± 0.2 mV and $(1.40 \pm 0.06) \times 10^{-1}$ cm s^{-1} respectively with α pinned at 0.50. However, the results of this study indicate that values of parameters reported can be a function of the data analysis method employed.

The FTAC harmonic based method implemented in the MLE-ExpHarmPer context has advantages of enhanced electrode kinetic sensitivity and minimisation of the contribution from the background current and provides noise reduction. Advantages of the total (AC + DC) current based MLE-TCDS method include shorter computation times, inferred posterior distributions are more accurate for parameter estimations in situations where the posteriors for each experiment do not overlap and calculation of the experimental noise present also is straightforward. This method is predicted to be as successful as the MLE-ExpHarmPer one for parameterisation of processes with electrode kinetics which are slower than for the $[Fe(CN)_6]^{3-/4-}$ process at a gold electrode and could approach that for the presently considered system if a higher frequency sine wave is applied in the AC voltammetric experiment. Both these scenarios will provide data regimes that are well removed for the reversible limit.

In general terms, it needs to be recognised that parameters reported from analysis of voltammetric

experiment can be a function of the data analysis method. The solution to the forward problem using sophisticated models and simulations is well advanced. However, methods and protocols for reliably solving the inverse problem in a statistical framework still need significant investigation.[53,66] This work confirms that Bayesian inference approaches are powerful, but need to be implemented with caution. Indeed their automated introduction without careful scrutiny of the fidelity of parameters recovered is fraught with danger. For this reason, before more intelligent automated methods are developed, heuristic methods accompanied with visual inspection of simulated and experimental data comparisons still should be used where possible to detect model deficiencies and related data estimation issues as well as provide guidance to and understanding of the advantages and disadvantages of different parameterisation methods.

9 Supporting Information

The fitted harmonic comparisons for the experimental data shown in Table 5 are provided in the Supporting Information. Multiple parameter posterior distribution histograms and kernel density plots for correlation of parameters calculated via the MCMC method calculations are also contained in the Supporting Information.

Acknowledgements

The authors gratefully acknowledge Dr Si-Xuan Guo for helpful discussion. Jie Zhang, Alan M. Bond and David Gavaghan would also like to thank the Australian Research Council for financial support provided by the award of a Discovery Grants DP170101535 and DP210100606.

Conflict of Interest

The authors declare no conflict of interest.

References

[1] Savéant, J.-M.; Costentin, C. *Elements of Molecular and Biomolecular Electrochemistry*; Wiley, 2019.

[2] Bard, A. J.; Faulkner, L. R. *Electrochemical Methods*; John Wiley & Sons Inc, 2000.

[3] Compton, R. G.; Banks, C. E. *Understanding Voltammetry*; IMPERIAL COLLEGE PRESS, 2010.

[4] Rudolph, M.; Reddy, D. P.; Feldberg, S. W. *Analytical Chemistry* **1994**, *66*, 589A–600A.

[5] Amatore, C.; Klymenko, O.; Svir, I. *Electrochemistry Communications* **2010**, *12*, 1170–1173.

[6] AB, C. COMSOL Multiphysics® v. 5.4., Stockholm, Sweden. 2018.

[7] Kennedy, G. F.; Bond, A. M.; Simonov, A. N. *Current Opinion in Electrochemistry* **2017**, *1*, 140–147.

[8] Li, J.; Kennedy, G. F.; Gundry, L.; Bond, A. M.; Zhang, J. *Analytical Chemistry* **2019**, *91*, 5303–5309.

[9] Rahman, M. A.; Gundry, L.; Ueda, T.; Bond, A. M.; Zhang, J. *The Journal of Physical Chemistry C* **2020**, *124*, 16032–16047.

[10] Rahman, M. A.; Li, J.; Guo, S.-X.; Kennedy, G.; Ueda, T.; Bond, A. M.; Zhang, J. *Journal of Electroanalytical Chemistry* **2020**, *872*, 113786, Dr. Richard Compton 65th birthday Special issue.

[11] Bond, A. M.; Elton, D.; Guo, S.-X.; Kennedy, G. F.; Mashkina, E.; Simonov, A. N.; Zhang, J. *Electrochemistry Communications* **2015**, *57*, 78–83.

[12] Bieniasz, L. K. *Journal of Electroanalytical Chemistry* **1996**, *406*, 45–52.

[13] Bieniasz, L.; Speiser, B. *Journal of Electroanalytical Chemistry* **1998**, *458*, 209–229.

[14] Bieniasz, L. K.; Rabitz, H. *Analytical Chemistry* **2006**, *78*, 8430–8437.

[15] Gavaghan, D. J.; Cooper, J.; Daly, A. C.; Gill, C.; Gillow, K.; Robinson, M.; Simonov, A. N.; Zhang, J.; Bond, A. M. *ChemElectroChem* **2017**, *5*, 917–935.

[16] Robinson, M.; Simonov, A. N.; Zhang, J.; Bond, A. M.; Gavaghan, D. *Analytical Chemistry* **2018**, *91*, 1944–1953.

[17] Gelman, A.; Rubin, D. B. *Statistical Science* **1992**, *7*, 457–472.

[18] Bond, A. M.; Duffy, N. W.; Guo, S.-X.; Zhang, J.; Elton, D. *Analytical Chemistry* **2005**, *77*, 186 A–195 A.

[19] Guo, S.-X.; Bond, A. M.; Zhang, J. *Review of Polarography* **2015**, *61*, 21–32.

[20] Zouraris, D.; Dimarogona, M.; Karnaouri, A.; Topakas, E.; Karantonis, A. *Bioelectrochemistry* **2018**, *124*, 149–155.

[21] Zouraris, D.; Karantonis, A. *Journal of Electroanalytical Chemistry* **2019**, *847*, 113245.

[22] Muraleedharan, M. N.; Zouraris, D.; Karantonis, A.; Topakas, E.; Sandgren, M.; Rova, U.; Christakopoulos, P.; Karnaouri, A. *Biotechnology for Biofuels* **2018**, *11*.

[23] Guin, S. K.; Ambolikar, A. S.; Das, S.; Poswal, A. K. *Electroanalysis* **2020**, *32*, 1629–1641.

[24] Song, P.; Ma, H.; Meng, L.; Wang, Y.; Nguyen, H. V.; Lawrence, N. S.; Fisher, A. C. *Physical Chemistry Chemical Physics* **2017**, *19*, 24304–24315.

[25] Elbaz, L.; Friedman, A. *ECS Meeting Abstracts* **2020**, *MA2020-02*, 2172–2172.

[26] Harris, A. R.; Newbold, C.; Cowan, R.; Wallace, G. G. *Journal of The Electrochemical Society* **2019**, *166*, G131–G140.

[27] Morris, G. P.; Simonov, A. N.; Mashkina, E. A.; Bordas, R.; Gillow, K.; Baker, R. E.; Gavaghan, D. J.; Bond, A. M. *Analytical Chemistry* **2013**, *85*, 11780–11787.

[28] Házì, J.; Elton, D. M.; Czerwinski, W. A.; Schiewe, J.; Vicente-Beckett, V. A.; Bond, A. M. *Journal of Electroanalytical Chemistry* **1997**, *437*, 1–15.

[29] Simonov, A. N.; Mashkina, E.; Mahon, P. J.; Oldham, K. B.; Bond, A. M. *Journal of Electroanalytical Chemistry* **2015**, *744*, 110–116.

[30] Kurtzer, G. M.; Sochat, V.; Bauer, M. W. *PLOS ONE* **2017**, *12*, e0177459.

[31] Oliphant, T. E. *A guide to NumPy*; Trelgol Publishing USA, 2006; Vol. 1.

[32] Bond, A. M.; Duffy, N. W.; Elton, D. M.; Fleming, B. D. *Analytical Chemistry* **2009**, *81*, 8801–8808.

[33] Haario, H.; Saksman, E.; Tamminen, J. *Bernoulli* **2001**, *7*, 223.

[34] Johnstone, R. H.; Chang, E. T.; Bardenet, R.; de Boer, T. P.; Gavaghan, D. J.; Pathmanathan, P.; Clayton, R. H.; Mirams, G. R. *Journal of Molecular and Cellular Cardiology* **2016**, *96*, 49–62.

[35] Johnstone, R. H.; Bardenet, R.; Gavaghan, D. J.; Mirams, G. R. *Wellcome Open Research* **2016**, *1*, 6.

[36] Hansen, N. *Towards a new evolutionary computation*; Springer, 2006; pp 75–102.

[37] Elgrishi, N.; Rountree, K. J.; McCarthy, B. D.; Rountree, E. S.; Eisenhart, T. T.; Dempsey, J. L. *Journal of Chemical Education* **2017**, *95*, 197–206.

[38] Abramson, D.; Bethwaite, B.; Enticott, C.; Garic, S.; Peachey, T. *IEEE Transactions on Parallel and Distributed Systems* **2011**, *22*, 960–973.

[39] Mashkina, E.; Bond, A. M.; Simonov, A. N. *Australian Journal of Chemistry* **2017**, *70*, 990.

[40] Simonov, A. N.; Morris, G. P.; Mashkina, E.; Bethwaite, B.; Gillow, K.; Baker, R. E.; Gavaghan, D. J.; Bond, A. M. *Analytical Chemistry* **2016**, *88*, 4724–4732.

[41] Simonov, A. N.; Grosse, W.; Mashkina, E. A.; Bethwaite, B.; Tan, J.; Abramson, D.; Wallace, G. G.; Moulton, S. E.; Bond, A. M. *Langmuir* **2014**, *30*, 3264–3273.

[42] Simonov, A. N.; Morris, G. P.; Mashkina, E. A.; Bethwaite, B.; Gillow, K.; Baker, R. E.; Gavaghan, D. J.; Bond, A. M. *Analytical Chemistry* **2014**, *86*, 8408–8417.

[43] Clerx, M.; Robinson, M.; Lambert, B.; Lei, C. L.; Ghosh, S.; Mirams, G. R.; Gavaghan, D. J. *Journal of Open Research Software* **2019**, *7*.

[44] Robinson, M.; Ounnunkad, K.; Zhang, J.; Gavaghan, D.; Bond, A. *ChemElectroChem* **2018**, *5*, 3771–3785.

[45] Adamson, H.; Bond, A. M.; Parkin, A. *Chemical Communications* **2017**, *53*, 9519–9533.

[46] Robinson, M.; Ounnunkad, K.; Zhang, J.; Gavaghan, D.; Bond, A. M. *ChemElectroChem* **2019**, *6*, 5499–5510.

[47] Sher, A. A.; Bond, A. M.; Gavaghan, D. J.; Harriman, K.; Feldberg, S. W.; Duffy, N. W.; Guo, S.-X.; Zhang, J. *Analytical Chemistry* **2004**, *76*, 6214–6228.

[48] Mathews, J. H.; Matthews, J.; Howell, R. W. *Complex Analysis For Mathematics And Engineering*; Jones & Bartlett Pub, 1997.

[49] Fleming, B. D.; Zhang, J.; Bond, A. M.; Bell, S. G.; Wong, L.-L. *Analytical Chemistry* **2005**, *77*, 3502–3510.

[50] Mashkina, E. A.; Simonov, A. N.; Bond, A. M. *Journal of Electroanalytical Chemistry* **2014**, *732*, 86–92.

[51] Li, J.; Bentley, C. L.; Bond, A. M.; Zhang, J. *Analytical Chemistry* **2016**, *88*, 2367–2374.

[52] Tan, Y.; Stevenson, G. P.; Baker, R. E.; Elton, D.; Gillow, K.; Zhang, J.; Bond, A. M.; Gavaghan, D. J. *Journal of Electroanalytical Chemistry* **2009**, *634*, 11–21.

[53] Gundry, L.; Guo, S.-X.; Kennedy, G.; Keith, J.; Robinson, M.; Gavaghan, D.; Bond, A. M.; Zhang, J. *Chemical Communications* **2021**, *57*, 1855–1870.

[54] Li, J.; Guo, S.-X.; Bentley, C. L.; Bano, K.; Bond, A. M.; Zhang, J.; Ueda, T. *Electrochimica Acta* **2016**, *201*, 45–56.

[55] Bracewell, R. *The Fourier Transform & Its Applications*; McGraw-Hill Science/Engineering/Math, 1999.

[56] Zhang, J.; Guo, S.-X.; Bond, A. M. *Analytical Chemistry* **2007**, *79*, 2276–2288.

[57] Li, J.; Bentley, C. L.; Ueda, T.; Bond, A. M.; Zhang, J. *Journal of Electroanalytical Chemistry* **2018**, *819*, 193–201.

[58] yin Tan, S.; Unwin, P. R.; Macpherson, J. V.; Zhang, J.; Bond, A. M. *Analytical Chemistry* **2017**, *89*, 2830–2837.

[59] Beriet, C.; Pletcher, D. *Journal of Electroanalytical Chemistry* **1993**, *361*, 93–101.

[60] Bano, K.; Nafady, A.; Zhang, J.; Bond, A. M.; ul Haque, I. *The Journal of Physical Chemistry C* **2011**, *115*, 24153–24163.

[61] Peter, L.; Dürr, W.; Bindra, P.; Gerischer, H. *Journal of Electroanalytical Chemistry and Interfacial Electrochemistry* **1976**, *71*, 31–50.

[62] Iwasita, T.; Schmickler, W.; Herrmann, J.; Vogel, U. *Journal of The Electrochemical Society* **1983**, *130*, 2026–2032.

[63] Randles, J. E. B.; Somerton, K. W. *Trans. Faraday Soc.* **1952**, *48*, 937–950.

[64] Daum, P. H.; Enke, C. G. *Analytical Chemistry* **1969**, *41*, 653–656.

[65] Heyrovsky, J. *Principles of polarography*; Pub. House of Czechoslovak Academy of Sciences Academic Press: Prague New York, 1966.

[66] Bond, A. M. *Journal of Solid State Electrochemistry* **2020**, *24*, 2041–2050.

[67] Usov, P. M.; Simonov, A. N.; Bond, A. M.; Murphy, M. J.; D'Alessandro, D. M. *Analytical Chemistry* **2017**, *89*, 10181–10187.

Keywords

Voltammetry, Bayesian Inference, Parameterisation, Large Amplitude AC Voltammetry, Fourier Transformation

TOC

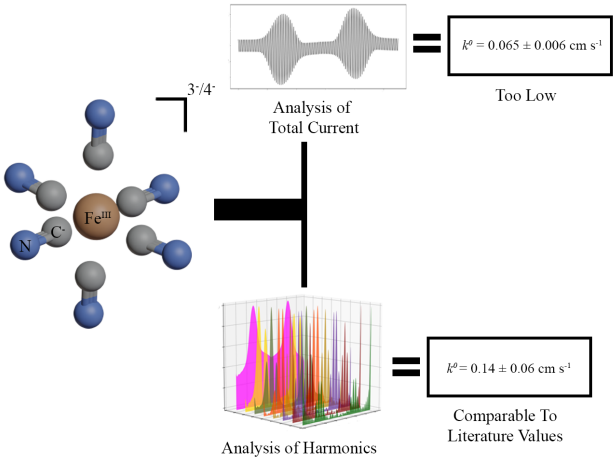

Automated Analysis: A range of Bayesian inference methods have been developed for parameterisation of large amplitude Fourier transformed AC voltammetric data. The advantages and limitations associated with each method were thoroughly assessed using both "noisy" synthetic and experimental data for the $[Fe(CN)_6]^{3-/4-}$ process in aqueous 3.0 M KCl electrolyte at a gold electrode.

Twitter Usernames: @JieZhang_Monash (Jie Zhang), @gundry_luke (Luke Gundry)